Highlighting nitrification disturbances in waters with high levels of nitrogen salts

Morgane Poser, Pascal Peu, Annabelle Couvert, Eric Dumont

Highlighting nitrification disturbances in waters with high levels of nitrogen salts

Morgane POSER[1,4], Pascal PEU[2], Annabelle COUVERT[1], Eric DUMONT[3*]

[1] Univ Rennes, Ecole Nationale Supérieure de Chimie de Rennes, CNRS, ISCR, UMR 6226, F-35000 Rennes, France

[2] INRAE, UR OPAALE, 17 avenue de Cucillé, CS 64427, 35 044 Rennes cedex, France

[3] Nantes Université, IMT Atlantique, CNRS, GEPEA, UMR 6144, F-44000, Nantes, France

[4] Agence de l'environnement et de la Maîtrise de l'Energie, 20 avenue du Grésillé, BP 90406, 49004 Angers Cedex 01, France

*Corresponding author: eric.dumont@imt-atlantique.fr

Abstract

Nitrification in extreme conditions was studied in a gas/liquid bioreactor treating gaseous ammonia (NH_3) emissions. As autotrophic bacteria can use simple inorganic compounds to supplement their energy requirements (i.e., NH_3 and carbon dioxide CO_2 from air), no nutrients or carbon sources were introduced into the water to support biomass growth. Furthermore, the continuous recirculation of water in a closed-loop within the bioreactor resulted in the accumulation of ammonium (NH_4^+), nitrite (NO_2^-), and nitrate (NO_3^-) concentrations in the water reaching levels in the order of several thousand milligrams per liter (mg L^{-1}). The bioreactor underwent continuous monitoring throughout four experiments, spanning a total duration of two years. The results unveil that unexplained yet reproducible phenomena occurred during the nitrification process: (1) once NH_4^+ and NO_2^- accumulated in the water, significant losses of these two nitrogen forms occurred simultaneously while maintaining the mass transfer of ammonia from the gas phase to the water; (2) continuous production of NO_3^- was observed despite the absence of nitrite oxidizing bacteria (NOB) due to inhibition phenomena induced by elevated concentrations of free ammonia (FA) and free nitrous acid (FNA); (3) sudden unidentified inputs of ionized nitrogen forms NH_4^+, NO_2^-, and NO_3^- occurred in the bioreactor. The findings and microbial analysis indicate that simultaneous nitrification denitrification (SND) process could occur in the bioreactor. However, this assumption is constrained by the unfavorable carbon to nitrogen ratio (C/N <1) and the negligible production of N_2O. To date, the surprising phenomena recorded in the bioreactor remain unresolved, indicating that certain mechanisms within the nitrogen cycle in challenging environments are still unknown.

Keywords

Ammonia, Nitrification, Nitrogen assimilation, Simultaneous nitrification denitrification, Bioreactors, Biofiltration

1. Introduction

Anthropogenic ammonia (NH_3) emissions contribute significantly to acid rain and acidification of ecosystems. Consequently, mass transfer and transformation of ammonia through oxidation are vital aspects in processes designed for the treatment of polluted air. Using environmental technologies like bioreactors for the purification of gaseous ammonia emissions involves the initial transfer of NH_3 into water, where it undergoes conversion into ammonium (NH_4^+). In water, the chemical balance between free ammonia (FA, i.e., $NH_{3,L}$) and ammonium is contingent upon both pH and temperature. Under aerobic conditions, NH_4^+ is oxidized into nitrite (NO_2^-) by ammonia-oxidizing bacteria (AOB) and ammonia-oxidizing archaea (AOA) then nitrate (NO_3^-) by nitrite-oxidizing bacteria (NOB). In bioreactors, this conventional nitrogen transformation process (autotrophic nitrification) results in the accumulation of three primary ionized nitrogen forms in water (NH_4^+, NO_2^-, and NO_3^-) which can be quantified by monitoring the increase in the electrical conductivity of the liquid (EC_L) [1–4]. Nitrification also induces biomass growth via NH_4^+ assimilation [5,6] and contributes to biofilm formation. Practically, as the water recirculates continuously in a closed-loop system without discharge, the cumulative nitrogen salt content in the water can reach levels in the range of several thousand milligrams of nitrogen per liter (mgN L^{-1}) and EC_L values up to 70 mS cm^{-1} are reported [4,7]. Nonetheless, the accumulation of nitrogen ions has significant inhibition effects on microorganisms, resulting in disruptions to the nitrification process [8–13] that require further elucidation. The presence of free ammonia in equilibrium with NH_4^+ exhibits inhibitory effects on both AOB and NOB, with AOB demonstrating higher tolerance compared to NOB [9]. Additionally, the presence of free nitrous acid (FNA, i.e., HNO_2) contributes to these inhibitory effects. Inhibitory effects disrupt the nitrification process, often resulting in substantial accumulations of NO_2^- in the water [1,2,14]. However, a contrasting phenomenon is also noted, where NO_2^- concentrations may occasionally be markedly lower than NO_3^- concentrations [2,3]. This could stem from the activity of comammox bacteria (COMplete AMMonia OXidation), which have the capability to fully oxidize NH_4^+ to NO_3^- [15,16]. Additionally, the role of heterotrophic nitrifiers, which rely on organic compounds as their energy source, in contrast to the chemolithotrophic nitrifiers, must also be considered. However, the limited knowledge about heterotrophic nitrification limits the understanding of nitrogen oxidation in the nitrogen cycle [17]. Throughout the nitrification process, the production and release of nitrous oxide (N_2O), an environmentally detrimental greenhouse gas contributing to climate warming [18], may also occur [2,3,19,20]. In bioreactors designed for treating ammonia emissions from livestock, it was observed that as much as 5% of the transferred ammonia to water could be transformed into N_2O [3]. This suggests the potential occurrence of an aerobic denitrification process within these apparatus. Consequently, it is challenging to assert that every ammonia transferred from the gas phase to water in aerobic bioreactors is exclusively retained in ionized forms (NH_4^+, NO_2^- and NO_3^-), used for biomass growth or solely emitted as N_2O. Attempts carried out to check the nitrogen mass balance in these bioreactors evidenced that balances could not be closed [3,4,21], suggesting probable nitrogen emissions or sinks. It was thereby hypothesized that unaccounted nitrogen might be emitted as N_2 produced by nitrifying bacteria [4] although this assertion requires further confirmation. Under oxygen limitation, such as in deep zones of the biofilm poorly oxygenated [22], autotrophic nitrifiers are able to reduce NO_2^- to NO, N_2O or N_2 [23]. Furthermore, recent findings have unveiled a novel denitrification pathway known as oxygenic denitrification, which involves the enzymatic reduction of NO_2^- to nitric oxide (NO), followed by the production of N_2 and O_2 [24]. This new pathway avoids the production of N_2O as an intermediate in

the reduction of NO. Therefore, it becomes evident that there are still gaps in our understanding of nitrogen transformations within bioreactors, and the impact of the accumulated nitrogen ions in water on nitrification disturbances remains largely unexplored. For instance, unforeseen and unexplained significant decreases in the electrical conductivity of the water were observed in industrial plants, which suggests that the nitrogen salt content in the water was decreasing during the treatment of gaseous ammonia emissions in spite of ammonia removal (unpublished data). In other words, it is plausible that a significant part of the ionized nitrogen forms (NH_4^+, NO_2^-, and NO_3^-) are transformed into other nitrogen forms, which are either reemitted into the atmosphere or accumulated in the water as unionized forms. Consequently, there is a need to carry out new investigations to enhance our understanding of nitrogen transformation in water with high salt content.

Studies on ammonia nitrification in bioreactors designed for treating gaseous emissions are usually carried out on pilot plants situated in intensive livestock. In these setups, continuous and accurate measurements of operating parameters and nitrogen salt content pose challenges, especially during long-term experiments. Therefore, the objective of this study was to conduct laboratory-scale experiments under controlled conditions, aiming to establish the nitrogen mass balance of a bioreactor operating continuously over an extended period. The goal was to gain a deeper understanding of the impact of elevated nitrogen salt content on the nitrification process. The objective involved working under severe conditions, particularly concerning nitrogen salt content (up to several g L^{-1}) and nutrients levels, as autotrophic bacteria can derive energy from simple inorganic compounds. The study focused on the nitrification process through four extended experiments, each lasting between 3-6 months. Importantly, the water remained unchanged during each experiment, with only tap water additions used to offset evaporative losses, mirroring real industrial plant conditions. Over the course of the two-year experiment duration, the bioreactor underwent continuously monitoring, encompassing measurements of temperature, NH_3 and N_2O concentrations in the gas phase at both inlet and outlet points, and measurements of temperature, pH, electrical conductivity, and NH_4^+, NO_2^- and NO_3^- concentrations in the water. Additionally, samples of biofilm, sludges and water were consistently extracted from the apparatus to track the evolution of the microbial community over time.

2. Material and methods

2.1. Experimental setup and operating conditions

The four experiments were carried out using a pilot-scale bioreactor, illustrated in Figure 1, comprising a cylindrical plastic column (0.305 m inlet diameter) filled with a channel-structured polypropylene packing material (WAT NET 150 NC 20/48 from WaluTech, Germany; packing height: 1.15 m; packing volume: $V_{packing\ material}$ = 0.084 m^3; specific surface area: 125 $m^2\ m^{-3}$) and a hermetically closed tank (volume 100 L; water volume V_L = 80 L). Gaseous ammonia emissions were generating by blending a clean air stream from a centrifugal air fan (VCP HP 75 Europe Environment, France) with pure ammonia gas from a NH_3 storage tank. The flow-rate of pure ammonia gas was regulated using a mass flow meter (Bronkhorst, Leonhardsbuch, Germany). Water in the bioreactor was consistently circulated using a centrifugal pump (SERMES, Netherlands). Given the ongoing evaporation of the water, tap water was added daily to uphold a constant level in the storage tank. The average properties of tap water were as follows: pH = 8.0-8.8; electrical conductivity = 0.42 mS cm^{-1}; Cl^- = 57 mg L^{-1}; Na^+ = 34.2 mg L^{-1}; SO_4^{2-} = 6.6 mg L^{-1}; NO_3^- = 4.1 mg L^{-1}. The temperature and pH of the water were measured but not controlled. To prevent ammonia mass transfer limitations in the bioreactor resulting from hydrodynamic conditions, the operating conditions summarized in Table 1 were applied throughout all experiments. At the beginning of experiments EXP 1 and EXP 3 (Table 1),

the water was inoculated with 10 L of activated sludge from a wastewater treatment plant (Procanar, Lauzach, France). Between each experiment, the saline water was discharged and replaced with fresh tap water. Throughout the entire experiments, no nutritive solution was added, as autotrophic bacteria could rely on simple inorganic compounds like NH_3 and CO_2 to fulfill their energy needs. Consequently, apart from the continuous supply of CO_2 from the air and the two one-time additions of organic carbon during water inoculation, no additional carbon source was added during the experiments.

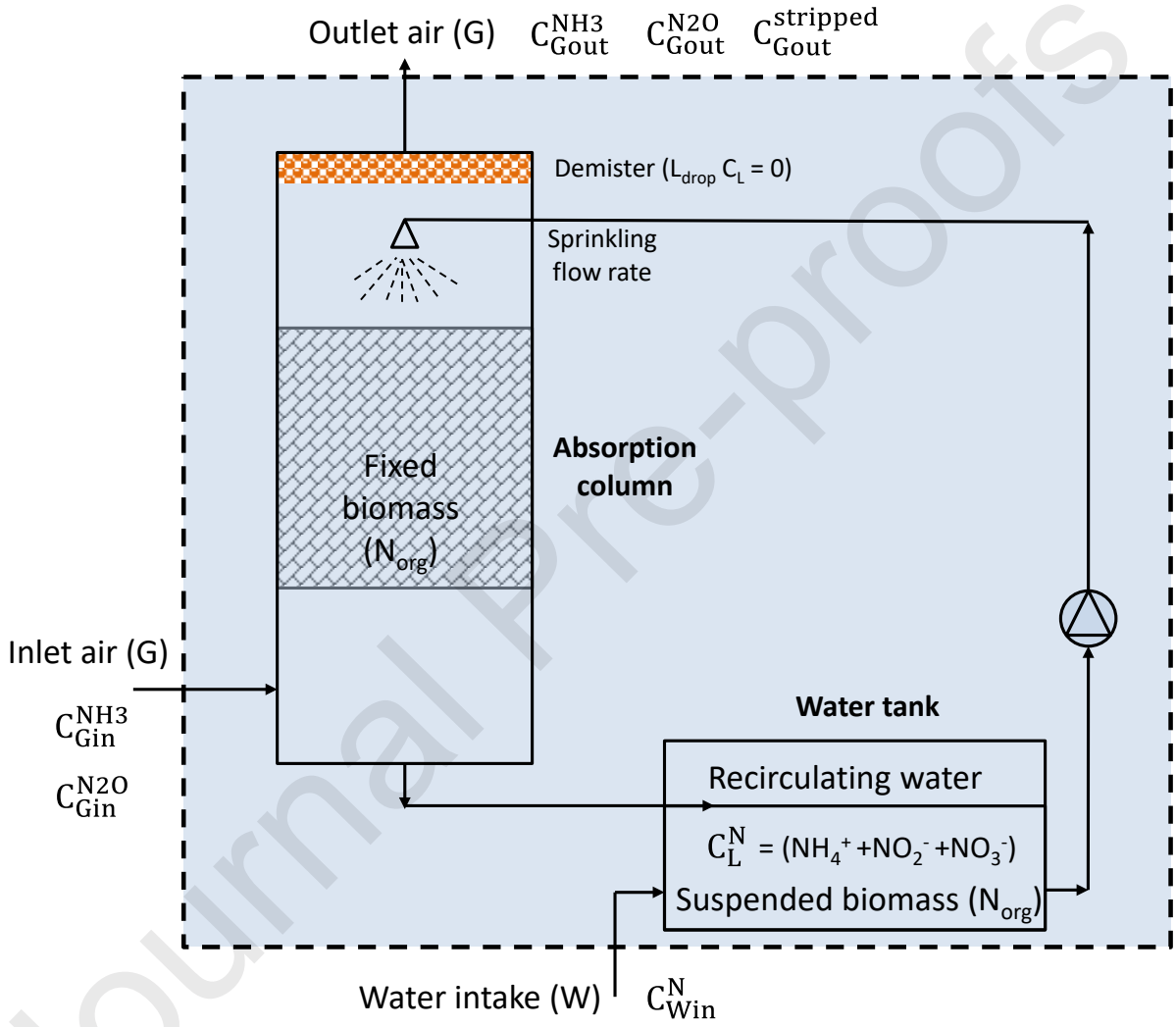

Figure 1 Overview of the bioreactor for the ammonia treatment (packed absorption column and water tank) and parameters used for the nitrogen mass balance

Table 1 Operating conditions

	EXP 1	**EXP 2**	**EXP 3**	**EXP 4**
Start	January 5, 2021	July 22, 2021	February 28, 2022	August 30, 2022
End	July 19, 2021	December 21, 2021	July 13, 2022	December 16, 2022
Duration (days)	195	152	135	108
Biomass inoculation	Yes	No	Yes	No
Air flow rate ($m^3\ h^{-1}$)	105 ± 5	102 ± 5	92 ± 5	94 ± 5
Gas temperature (± 0.2°C)	17.3 – 27.2	16.9 – 27.3	18.5 – 32.2	19.2 – 29.1
Gas residence time[(a)] (s)	2.5 ± 0.1	2.6 ± 0.1	2.9 ± 0.1	2.8 ± 0.1
Gas velocity[(b)] ($m\ s^{-1}$)	0.40 ± 0.02	0.38 ± 0.02	0.35 ± 0.02	0.35 ± 0.02
Maximum inlet NH_3 concentration ($mg_{NH3}\ m^{-3}$)	20.0 ± 0.4	29.9 ± 0.6	17.8 ± 0.4	20.5 ± 0.4
Maximum NH_3 loading rate[(c)] ($g_{NH3}\ m^{-3}\ h^{-1}$)	25.0 ± 1.5	35.8 ± 2.1	20.4 ± 1.2	22.7 ± 1.4

Liquid flow rate (L min^{-1})	2.5 ± 0.1	2.5 ± 0.1	2.6 ± 0.1	2.5 ± 0.1
Liquid temperature (± 0.2°C)	11.8 – 23.7	13.3 – 23.7	13.9 – 23.6	13.5 – 23.9
Sprinkling flow-rate[(d)] (m^3 h^{-1} m^{-2})	2.0 ± 0.1	2.0 ± 0.1	2.1 ± 0.1	2.5 ± 0.1
NH_3 absorption factor[(e)]	3.2 ± 0.8	3.2 ± 0.8	3.3 ± 0.8	3.3 ± 0.8
Average daily water intake (L day^{-1})	17.1 ± 0.1	14.8 ± 0.1	22.6 ± 0.1	15.1 ± 0.1

(a) Gas residence time = volume of the packing material / gas flow-rate.

(b) Gas velocity = gas flow-rate / column cross section.

(c) NH_3 loading rate = gas flow-rate x ammonia concentration / volume of the packing material.

(d) Sprinkling flow-rate = liquid flow-rate / column cross section.

(e) Ammonia absorption factor = (liquid flow rate / (gas flow rate x ammonia Henry constant)); ammonia Henry constant = C_G^{NH3} / C_L^{NH3} (dimensionless).

2.2. Nitrogen balance

For the bioreactor illustrated in Figure 1, the mass balance can be expressed as follows: Nitrogen entering the system = Nitrogen leaving the system + Nitrogen transferred from the gas phase and accumulated into the liquid phase + Nitrogen assimilated by the biomass (both attached to the packing material and suspended in the water). The system under consideration is the entire bioreactor, as delineated by the dashed rectangle in Figure 1. The equation is (in gN h^{-1}):

$$G\,C_{Gin}^{NH3} + G\,C_{Gin}^{N2O} + W\,C_{Win}^{N} = G\,C_{Gout}^{NH3} + G\,C_{Gout}^{N2O} + G\,C_{Gout}^{Nstripped} + L_{drop}C_L^N + \frac{dbiomass}{dt} + V_L\frac{dC_L^N}{dt} \quad \text{Equation 1}$$

The substantial amount of nitrogen entering and leaving the system in the form N_2 was excluded from consideration since it cannot be absorbed into water due to: (i) the brief contact time between the gas phase and the liquid phase in the bioreactor (around 1-2 s), (ii) the Henry's law constant of N_2 in water (Table 2). The potential production of N2 resulting from biological activity within the bioreactor, which was unavoidably stripped and re-emitted into the air, is considered through the term $C_{Gout}^{Nstripped}$. This term is also applied to account for the potential production of NO_X by the biological activity. In Figure 1, ($G\ C_{Gin}^{NH3}$) and ($G\ C_{Gout}^{NH3}$) are the gaseous ammonia mass flow rates entering and leaving the system respectively; ($G\ C_{Gin}^{N2O}$) and ($G\ C_{Gout}^{N2O}$) are the gaseous nitrous oxide mass flow rates entering and leaving the system, respectively; ($W\ C_{Win}^{N}$) is the nitrogen content in the water entering the system to compensate the evaporated water (with nitrate being the primary nitrogen ion in tap water); ($L_{drop}C_L^N$) is the mass flow rate of nitrogen substances potentially leaving the system through droplet entrainment; $\left(\frac{dbiomass}{dt}\right)$ is the rate of nitrogen consumption utilized for biofilm formation (including the growth of microorganisms and the production of extracellular polymeric substances (EPS) [25]) and the potential assimilation of inorganic nitrogen to organic nitrogen (N_{org}); and ($V_L\frac{dC_L^N}{dt}$) is the nitrogen mass flow rate accumulated in the water in the inorganic forms NH_4^+, NO_2^- and NO_3^-. Assuming that droplet entrainment was avoided by the presence of an efficient demister, Equation 1 can be reformulated as:

$$G\left(C_{Gin}^{NH3} - C_{Gout}^{NH3}\right) + G\left(C_{Gin}^{N2O} - C_{Gout}^{N2O}\right) + W\ C_{Win}^{N} = G\ C_{Gout}^{Nstripped} + \frac{dbiomass}{dt} + V_L\frac{dC_L^N}{dt} \qquad \text{Equation 2}$$

Apart from the inorganic species NH_4^+, NO_2^- and NO_3^-, the water also contained free ammonia (FA, i.e. $NH_{3,L}$), hydroxylamine (NH_2OH), free nitrous acid (FNA, i.e. HNO_2), nitric acid (HNO_3) and nitric oxide (NO). Considering the high Henry's law solubility of NO (Table 2), this nitrogen form was therefore stripped from the water and was also considered through the term $C_{Gout}^{Nstripped}$. On the contrary, hydroxylamine, free nitrous acid and nitric acid exhibit high solubility in water. Nonetheless, due to the absence of water renewal, the amount of inorganic nitrogen forms (NH_4^+, NO_2^- and NO_3^-) was notably greater than that of unionized nitrogen forms like FA, FNA, hydroxylamine and nitric acid. The main unionized element, FA, and FNA can be calculated using the following relationships [8,9,21]:

$$FA_{\left(\frac{mgN}{L}\right)} = \frac{NH_{4\left(\frac{mgN}{L}\right)}^{+}\ 10^{pH}}{10^{pH} + \exp\left(\frac{6344}{273 + T_{(°C)}}\right)} \qquad \text{Equation 3}$$

$$FNA_{\left(\frac{mgN}{L}\right)} = \frac{NO_{2\left(\frac{mgN}{L}\right)}^{-}}{10^{pH}\exp\left(\frac{-2300}{273 + T_{(°C)}}\right)} \qquad \text{Equation 4}$$

In the typical pH range measured in bioreactors treating gaseous ammonia emissions (around neutrality [2]), the amount of FA is less than 1% of the NH_4^+ accumulated in water, and FNA is less than 0.1% of the NO_2^-.

Integrating Equation 2 with respect to time gives:

$$\left[G\left(C_{Gin}^{NH3} - C_{Gout}^{NH3}\right) + G\left(C_{Gin}^{N2O} - C_{Gout}^{N2O}\right) + W\,C_{Win}^{N}\right]\Delta t - V_L\,\Delta C_L^N = \Delta biomass + G\,C_{Gout}^{Nstripped}\,\Delta t \qquad \text{Equation 5}$$

Given that the left terms of Equation 5 are measured daily, it is possible to determine the overall amount of nitrogen used for biomass growth and the amount stripped from the bioreactor, i.e. re-emitted to the atmosphere (right terms).

Table 2 Henry's law solubility constants at 298.15 K [26]

Nitrogen form	**H (dimensionless)**
Ammonia (NH_3)	$6.84\ 10^{-4}$
Nitrogen (N_2)	63.1
Nitrous oxide (N_2O)	1.68
Nitric oxide (NO)	21.2
Nitrogen dioxide (NO_2)	2.88
Nitrogen trioxide (NO_3)	1.06
Nitrous acid (HNO_2)	$8.41\ 10^{-4}$
Nitric acid (HNO_3)	$1.92\ 10^{-7}$

Hydroxylamine (NH_2OH)	$2.88\ 10^{-7}$

2.3. Physico-chemical analysis of gas and liquid phases

Ammonia NH_3 and nitrous oxide N_2O in the gas phase at the inlet and outlet of the bioreactor were daily measured using a Fourier Transform InfraRed (FTIR) gas analyzer (GasmetTM DX-4030, Environment SA). The ammonia removal efficiency was subsequently calculated based on these continuous gaseous measurements:

$$\mathrm{RE}_{\mathrm{measured}} = 100\left(\frac{\mathrm{C}_{\mathrm{Gin}}^{\mathrm{NH3}} - \mathrm{C}_{\mathrm{Gout}}^{\mathrm{NH3}}}{\mathrm{C}_{\mathrm{Gin}}^{\mathrm{NH3}}}\right) \quad \text{Equation 6}$$

For water analysis, pH and electrical conductivity (EC_L) were measured using a multi-channel analyzer consort C834 (Consort bvba, Turnhout, Belgium) with temperature correction. Concentrations of inorganic nitrogen species, namely NH_4^+, NO_2^- and NO_3^-, were quantified through High Pressure Ion Chromatography (940 Professional IC Vario, Metrohm, conductivity detection, cation eluent: 3.2 mM Na_2CO_3 + 1 mM $NaHCO_3$, cation column: metrosep C4 250/4.0, anion eluent: 3.5 mM Na_2CO_3 + 3.0 mM $NaHCO_3$ + 10 % MeOH, anion column: Metrosep A Supp 5 150/4.0). Upon measuring the inlet ammonia concentration $\mathrm{C}_{\mathrm{Gin}}^{\mathrm{NH3}}$ (in $mg_{NH3}\ m^{-3}$), pH, liquid temperature and NH_4^+ in water (in $gN\ L^{-1}$), the predicted RE value, as determined by Dumont et al. [27], can be calculated using the following equation and subsequently compared with the measured value.

$$\mathrm{RE}_{\mathrm{predicted}} = 100\left(1 - \frac{17}{14}10^{6}\ \frac{\mathrm{H}\ \mathrm{NH}_4^+\ 10^{(-\mathrm{pK_a}+\mathrm{pH})}}{\mathrm{C}_{\mathrm{Gin}}^{\mathrm{NH3}}}\right) \quad \text{Equation 7}$$

2.4. Analysis of microbial community

Microbial community structures in the bioreactor were analyzed using samples collected during EXP 3. The samples included: (i) decanted sludges in the water tank (collected at days 0, 27, 69 and 151); (ii) biofilm extracted from the packing material at days 27 and 69; and (iii) water filtered at days 27, 69 and 151. All samples underwent centrifugation at 3000 g for 10 min, with subsequent removal of the supernatant. The resulting pellet was stored at – 20 °C until DNA extraction. DNA extraction was carried out using the Macherey Nagel NucleoSpin Soil kit. Microbial community dynamics were investigated through high throughput DNA sequencing employing Ion Torrent Personal Genome Machine methods and technologies (ThermoFisher ScientificLife Technologies, MA, USA), as outlined in Madigou et al. [28]. The analysis focused on the V4-V5 hypervariable regions of the bacterial and archaeal 16S rRNA genes through PCR amplification (Platinium SuperFi PCR protocol from Life

Technologies) and fusion primers 515F (5'- Ion A adapter–Barcode–GTGYCAGCMGCCGCGGTA-3'), 928R (5'-Ion trP1 adapter–CCCCGYCAATTCMTTTRAGT-3') and a specific primer for anammox 928Ramx bacteria (5'-CCCCGY-CAATTCHTTTRAGT-3') [29], incorporating a barcode and sequencing adapters. The resulting amplicons were purified and quantified using the Agencourt AMPure XP magnetic beads (Beckman Coulter), DNA 1000 kit and 2100 Bioanalyzer (Agilent Technologies), respectively. Template preparation for emulsion PCR and subsequent sequencing were performed using the Ion PGM Hi-Q View OT2 Kit and Ion PGM Hi-Q View Sequencing kit (Life Technologies) as described in [28]. The high-throughput DNA sequencing yielded an average of 3369/10071 ± 2291 sequence reads, each approximately 380 base pairs in length, for every sample. These sequences underwent processing using the FROGS pipeline [30], adhering to the recommendations provided by the authors on the MIGALE Galaxy instance (INRAE, Jouy-en-Josas, France). Abundance of Operational Taxonomic Unit (OTUs) and calculations of microbial community diversity indices were performed using Easy16S, a shiny web interface accessible at https://shiny.migale.inrae.fr/app/easy16S (accessed on 7 April 2022), which is based on the phyloseq R package [31]. The investigation of principal OUTs recovered in samples was used to predict nitrogen functional metabolism through marker genes mapped to the Kyoto Encyclopedia of Genes and Genomes (KEGG) database [32].

3. Results

The ammonia removal efficiency ($RE_{measured}$) and time changes in pH and electrical conductivity (EC_L) of water are depicted in Figure 2. Considering first EXP 1, the analysis of experimental results highlights several surprising findings.

During the biomass acclimatization period, the bioreactor demonstrated the capability to absorb ammonia from the initial days of operation, even under alkaline conditions that are typically unfavorable for ammonia mass transfer (pH = 8.8±0.1). In the initial 30 days, $RE_{measured}$ ranged from 20 to 30±6%, while the predicted RE values calculated from Equation 7 were 0. The main issue is that a large amount of the transferred ammonia was not found in the water. Thus, by day 32, the cumulative amount of NH_3 transferred from the gas reached 257±10 gN, whereas only 42±4 gN were measured in the water, in the forms NH_4^+, NO_2^- and NO_3^- due to the gradual start of nitrification. This finding suggests that the ammonia transferred from the gas was dissolved into various nitrogen forms, likely including free ammonia in equilibrium with NH_4^+. However, the FA concentration calculated from Equation 3 clearly indicated that the FA amount in the water was around 3.2±0.4 gN only. Consequently, it is challenging to explain where the missing nitrogen is, and in what forms it exists. This observation was already reported in the literature through studies carried out under similar operating conditions and using the same pilot [27,33], as well as in an industrial setting [7]. However, no satisfactory explanation has been suggested to describe this phenomenon.

After the biomass acclimatized, nitrification begun and the pH decreased from 8.8±0.1 (tap water value) to 7.4±0.1 (from day 42). As soon as the pH decreased, $RE_{measured}$ reached around 80±5%, indicating that large amounts of ammonia were transferred from gas to water. The rapid accumulation of NH_4^+ in the water, and its subsequent oxidation into NO_2^- by nitrifying bacteria, led to a quick increase in the electrical conductivity of water. Considering that the measured EC_L value accounted for both the ionized species forms coming from tap water and those resulting from the ammonia mass transfer in water and subsequent nitrification, the EC_L value was recalculated to remove the contribution of electrical conductivity from tap water (EC_L corrected). As depicted in Figure 2, the gap between the measured EC_L value and the corrected EC_L value logically widened over time (up to 10 mS cm^{-1} at the end of EXP 1). By day 51, EC_L reached 22.0±0.2 mS cm^{-1} and given that elevated EC_L values impede ammonia mass transfer [27], $RE_{measured}$ therefore decreased as rapidly as

it had increased, converging towards 20±2% by day 66. At this time, EC_L reached its maximum value, i.e. 69.7±0.7 mS cm^{-1}. Although this value may appear elevated, it is consistent with results occasionally achieved in industrial conditions [7], and the continuous evolution of EC_L does not indicate measurement errors. Nevertheless, the substantial increase in EC_L recorded between days 60 and 66 (rising from 35.7±0.4 to 62.1±0.6 mS cm^{-1}) is surprising and difficult to explain.

One of the most notable and unexpected findings from EXP 1 is the continuous decrease in EC_L observed from day 74, despite the fact that $RE_{measured}$ remained constant at 20±2%. In other words, the bioreactor demonstrated the simultaneous capacity to absorb ammonia from gas to water and remove ionic species dissolved in the water, presenting a seeming contradiction, unless one considers the possibility of a substantial emission of gaseous nitrogenous forms other than NH_3 and N_2O into the atmosphere (i.e. N_2 or NO_x). To explore this, three disruptions in the inlet ammonia concentration were then applied (initial increase up to 20.0±0.4 mg m^{-3}, subsequent decrease to 7.0±0.2 mg m^{-3}, and a final increase to 15.0±0.3 mg m^{-3}). However, these disruptions had no effect on changes in $RE_{measured}$ values, nor did they halt the decrease in EC_L.

The unexpected findings observed during EXP 1 are confirmed by EXP 2, 3 and 4 with marginal differences among them (Figure 2). Between EXP 1 and 2, the saline water was discharged and replaced with fresh water, which explains that the pH was 8.8±0.1 at the beginning of EXP 2. As the biomass had already acclimatized, nitrification rapidly started as indicated by the pH drop and the rapid increase in $RE_{measured}$. With the NH_3 inlet concentration set at 29.0±0.6 mg m^{-3}, a substantial quantity of ammonia was transferred to the water, consequently leading to a rapid increase in EC_L, up to 45.6±0.5 mS cm^{-1}. Similar to EXP 1, an unexpected continuous decrease in EC_L was observed for EXP 2 (from day 26 to day 96), while $RE_{measured}$ fluctuated between 14 and 22±2%, even after the change in the NH_3 inlet concentration to 8.5±0.2 mg m^{-3}. From day 96, $RE_{measured}$ notably increased to around 40±3%, then decreased, resulting in an EC_L increase from 23.0±0.3 to 32.0±0.3 mS cm^{-1}. A steady state was finally observed from day 128 to day 153 in terms of $RE_{measured}$, EC_L and pH values. At the beginning of EXP 3, salty water was replaced with fresh water which was inoculated since two months had elapsed between both experiments (Table 1). Although NH_3 inlet concentrations varied, results recorded during EXP 3 were similar to those achieved during EXP 2 in terms of EC_L and pH values. However, $RE_{measured}$ was slightly below 10±1% during the EC_L decrease period. In EXP 4, the experiment commenced with a very high $RE_{measured}$ value (90±6%) due to the pH of the fresh water being close to neutrality (7.5±0.1). Nevertheless, results recorded over time in EXP 4 were similar to those observed in the other experiments.

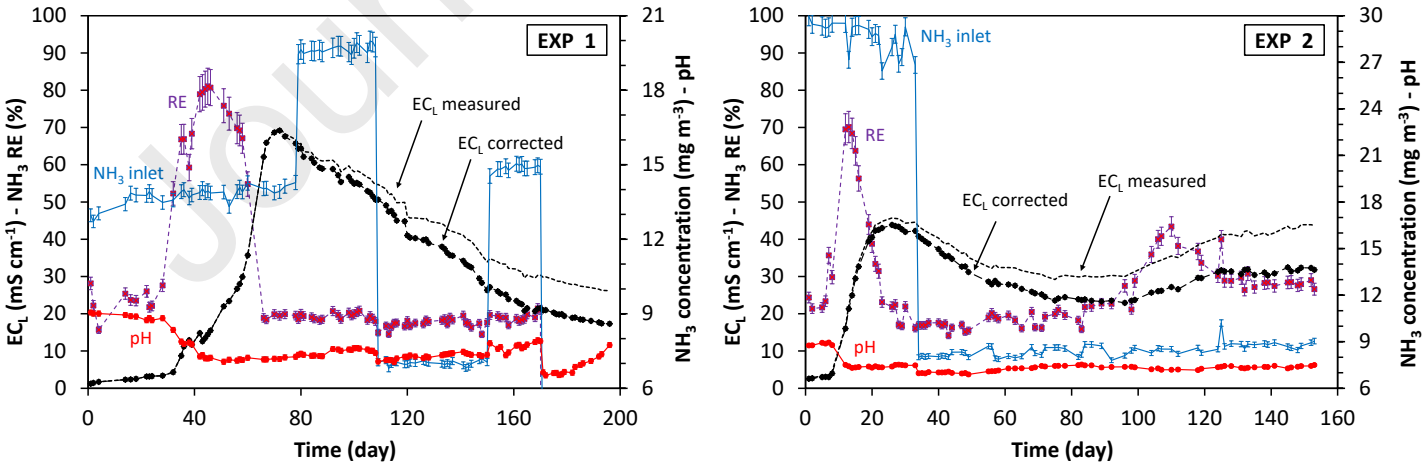

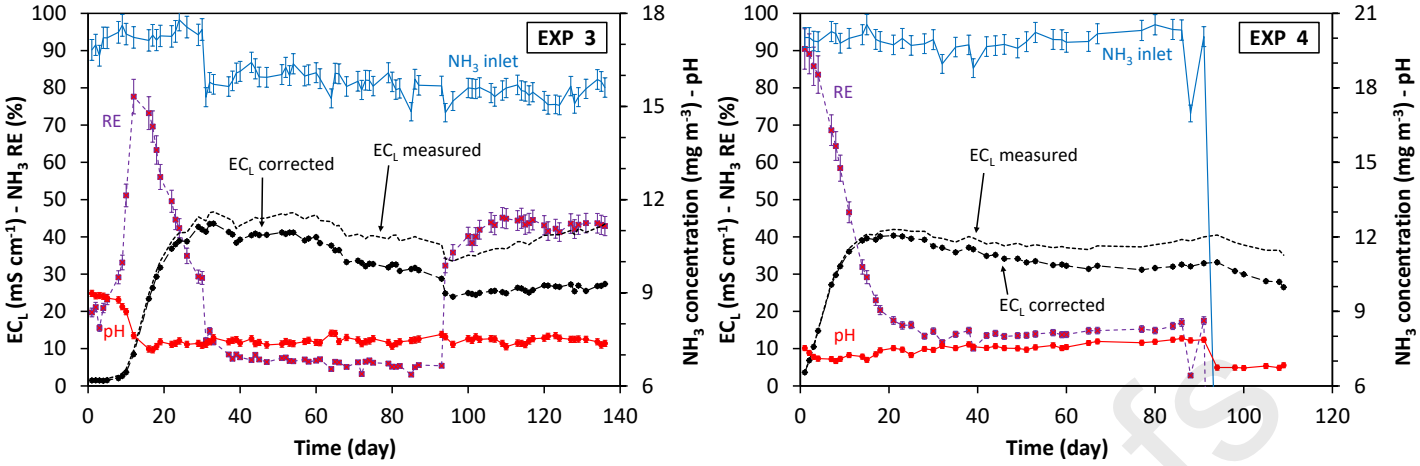

Figure 2 Key parameters recorded during the four experiments (ammonia concentration -NH_3 inlet-, pH, electrical conductivity of the washing liquid -EC_L measured and EC_L corrected to account for the presence of ionic species due to daily tap water intake- and ammonia removal efficiency - $RE_{measured}$ -)

Given that the change in EC_L over time is contingent upon the concentration of ionic species in water, primarily in the form of nitrogenous species NH_4^+, NO_2^- and NO_3^- resulting from the nitrification process, it can be concluded that the unexpected decreases in EC_L observed during EXP 1-4 are due to the depletion of these ionized nitrogen species in the water. This conclusion is confirmed by the measurements of NH_4^+, NO_2^- and NO_3^- concentrations over time, as depicted in Figure 3. Consequently, the EC_L decrease corresponds to similar decreases in NH_4^+ and NO_2^- concentrations, while NO_3^- concentration exhibited a continuous increase over time, albeit to a lesser extent. During the phases of decreasing EC_L, marked by the vertical dashed lines in Figure 3, the production rate of NO_3^-, as well as the loss rates of NH_4^+ and NO_2^- were satisfactorily modeled using linear equations. Results are summarized in Table 3. In all experiments, the nitrogen loss rates for NH_4^+ and NO_2^- are in the same order of magnitude (with a ratio $|NO_2^-/NH_4^+|$ around 1) and considerably higher than the production rate of NO_3^- (with a ratio $|NO_3^-/NH_4^+|$ around 0.2), except for EXP 4 where the production rate of NO_3^- is half of nitrogen loss rates for NH_4^+ and NO_2^-. Furthermore, nitrogen loss rates for NH_4^+ and NO_2^- exhibited a continuous decrease between EXP 1 and EXP 4. Ultimately, during the phases of decreasing EC_L, substantial amounts of nitrogen disappeared from the water (Table 3). In EXP 1, this amounted to 910±80 gN, and by the end of the experiment, 85% of the initially transferred ammonia from the gas phase had vanished from the water (Figure 4). This percentage was lower for the other experiments, either due to nitrogen accumulation occurring again in the water after the decreasing phase, as observed in EXP 2 and EXP 3 (44% and 37%, respectively), or due to low nitrogen loss rates for NH_4^+ and NO_2^-, as observed in EXP 4 (43%). To explain these findings, it can be speculated in a first approach that large amounts of NH_4^+ and NO_2^- in the water reacted chemically or biologically to form NO_3^- and nitrogen atmospheric forms, such as NO_X, N_2O or N_2, which then exited the bioreactor with the exhaust air (e.g. via oxygenic denitrification [24]). And the continuous nitrate formation observed in all four experiments should be due to the biological oxidation of the nitrite by the nitrite oxidizing bacteria (NOB). However, considering the high concentrations of NH_4^+ and NO_2^- in the water (reaching several thousand of mg L^{-1} each; Figure 3), the levels of inhibitors, such as free ammonia (FA) and free nitrous acid (FNA), were also substantial, as evidenced in Figure 5. According to the literature [9,11,34,35], FA concentrations inhibiting AOB range from 8 to 120 mgN L^{-1}, while NOB are much sensitive, with inhibition occurring at concentrations between 0.08 and 0.82 mgN L^{-1}. For all experiments, FA concentrations calculated from Equation 3 reached several dozen mgN L^{-1}, suggesting that NOB were likely fully inhibited, and consequently the presence of nitrate could not be attributed to NOB activity. Furthermore, the concentrations of FNA calculated from Equation 4, typically ranging between 0.2 and 1.0±0.1 mgN L^{-1} (as indicated by the horizontal blue dashed lines in

Figure 5), were sufficient to inhibit NOB (complete inhibition is observed for FNA concentrations > 1 mgN L^{-1} [35]). The high values of the NO_2^- accumulation ratio defined as $NO_2^-/(NO_2^-+NO_3^-)$ suggested a substantial degree of NOB inhibition [8] (with results ranging between 70 and 98% for all experiments). The absence of NOB was confirmed through the analysis of microbial diversity in the biomass harvested from the bioreactor, as will be demonstrated latter. FNA concentrations were also high enough to cause partial inhibition of AOB. Therefore, in such a severe environment and in the absence of NOB, it becomes challenging to attribute the biological production of NO_3^- solely to autotrophic nitrification. Given that the amount of NO_3^- from tap water addition was marginal in relation to the nitrate production rate (around 1-2%), it is likely that other chemical or biological mechanisms were involved.

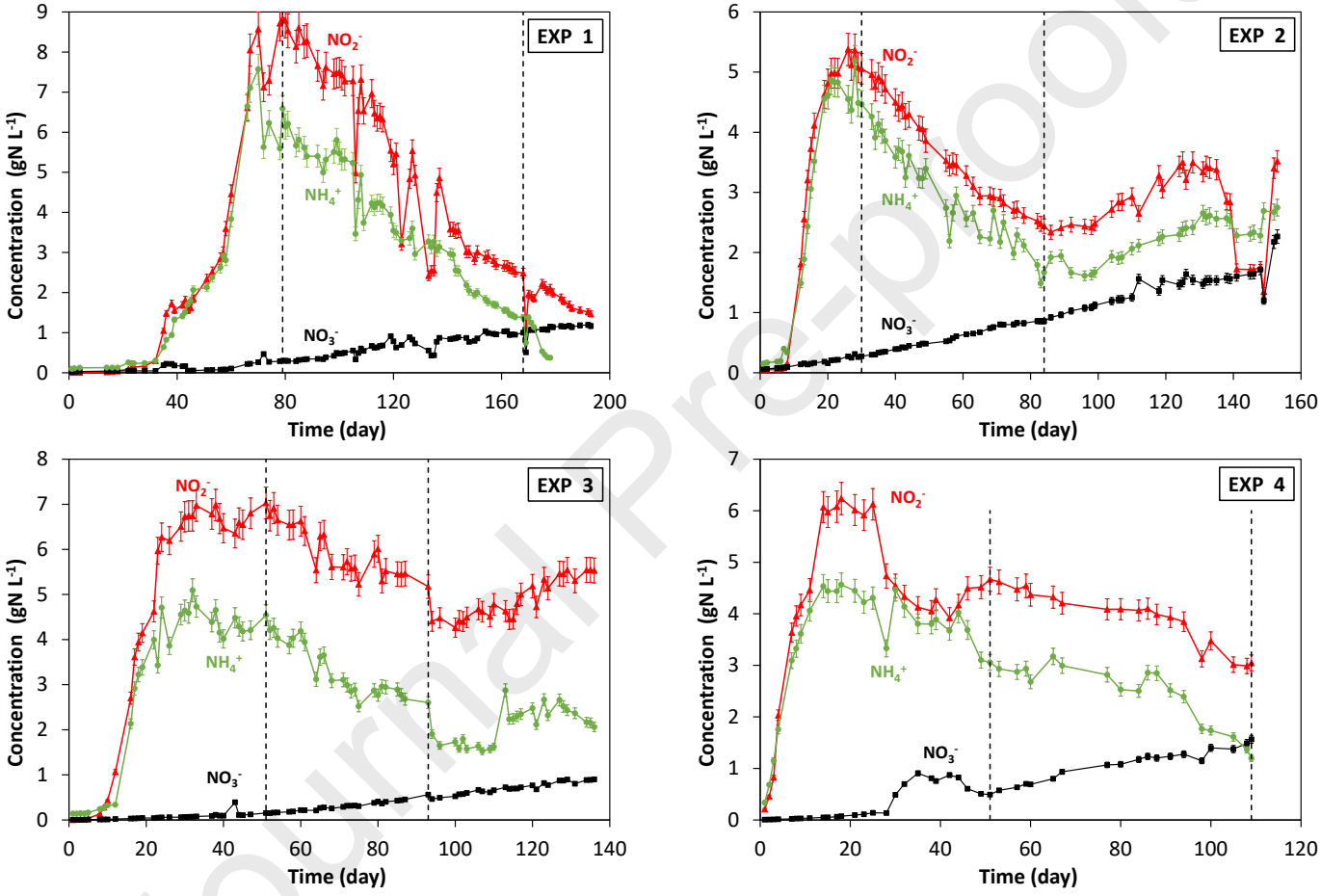

Figure 3 Concentrations of ammonium (NH_4^+), nitrite (NO_2^-) and nitrate (NO_3^-) measured in the water over the course of the four experiments

Table 3 Calculated average rates of nitrogen forms appearing and disappearing in the water during the phases of decreased electrical conductivity (EC_L)

		EXP 1	**EXP 2**	**EXP 3**	**EXP 4**
		Between days	Between days	Between days	Between days
		79 and 168	30 and 84	51 and 93	51 and 109
Nitrogen rate ($gN\ day^{-1}$)	Ammonium NH_4^+	- 4.5±0.2	- 3.8±0.2	- 3.7±0.2	- 2.2±0.2
	Nitrite NO_2^-	- 6.3±0.2	- 4.1±0.2	- 3.3±0.2	- 2.2±0.2
	Nitrate NO_3^-	+ 0.7±0.2	+ 0.9±0.2	+ 0.7±0.2	+ 1.3±0.2
Ratios	$\lvert NO_2^-/NH_4^+ \rvert$	1.39	1.07	0.90	1.00
	$\lvert NO_3^-/NH_4^+ \rvert$	0.15	0.24	0.19	0.60
Nitrogen "lost" during the period (gN)		910±80	375±30	264±21	175±14
Nitrogen "lost" per day ($mgN\ L^{-1}\ d^{-1}$)		128±13	87±8	79±8	38±4

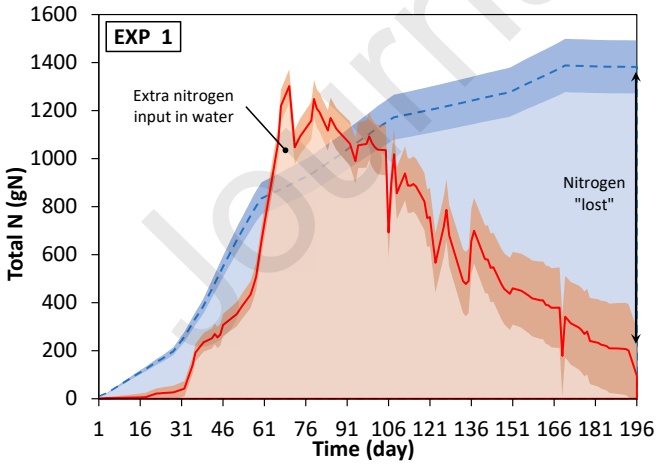

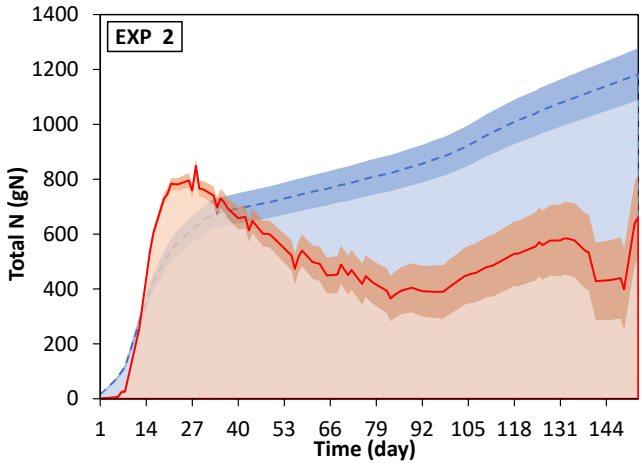

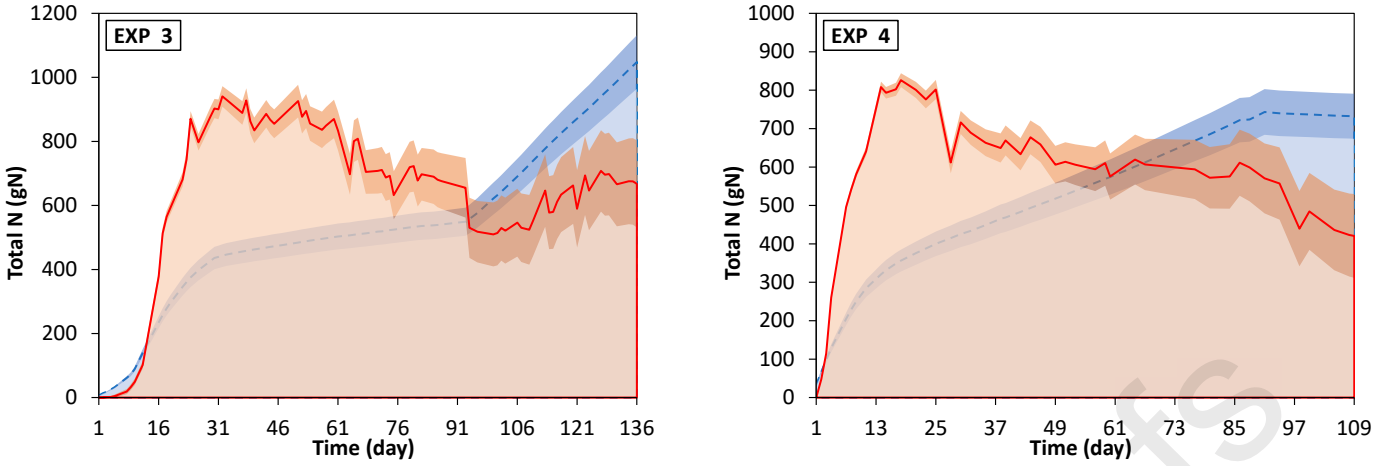

Figure 4 Cumulative amounts of nitrogen transferred into the bioreactor, i.e. $\left[G\left(C_{Gin}^{NH3}-C_{Gout}^{NH3}\right)+G\left(C_{Gin}^{N2O}-C_{Gout}^{N2O}\right)+W\,C_{Win}^{N}\right]\Delta t$ *(depicted by the blue dashed line) and nitrogen accumulated in the water as ammonium, nitrite and nitrate, i.e.* $V_L\,\Delta C_L^N$ *(red line). The shaded areas indicate measurement uncertainties. When the red line surpasses the blue dashed line, an additional input of nitrogen into the water occurs (according to Equation 5).*

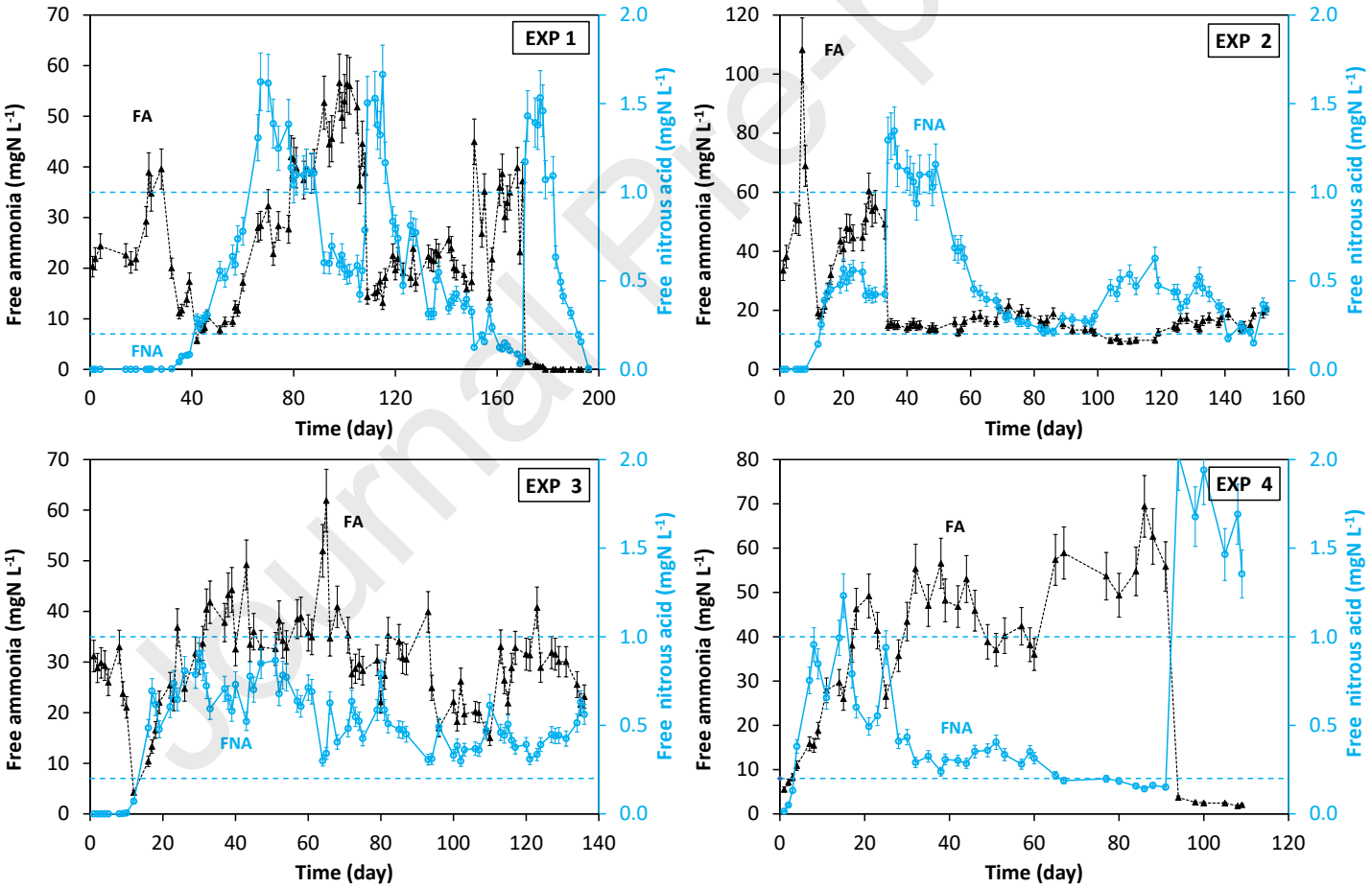

Figure 5 FA and FNA changes calculated over time from ammonium (NH_4^+) and nitrite (NO_2^-) concentrations in the water (Equation 3 and Equation 4). The horizontal blue dashed lines demarcate inhibition zones attributed to the presence FNA (partial NOB inhibition for FNA concentrations > 0.2 mgN L^{-1}; complete NOB inhibition for FNA concentrations > 1 mgN L^{-1} [35])

Another unexpected and surprising finding can be observed in Figure 4. Since the increase of the electrical conductivity of the water is attributed to the nitrogen transferred from the gas to the water (with consideration for the small amount of nitrogen present in the tap water), the cumulative amount of the ionized nitrogenous species in the water is expected to be lower, or at least equal, to the cumulative amount of nitrogen transferred from the gas phase to the water. The difference between these quantities corresponding to the nitrogen used for biomass growth or lost, as expressed by Equation 5. However, for EXP 1, a notable surprising change is observed by day 61. The measured amount of nitrogen in the water surpasses the amount transferred, indicating an additional input of nitrogen into the bioreactor. This phenomenon also appears for the three other experiments, albeit with more pronounced effects. Notably, the amount of nitrogen accumulated in the water exceeded the amount transferred by days 12 and 9 for EXP 2 and 3, respectively. The case of EXP 4 seems even more surprising since the amount of nitrogen accumulated in the water exceeded the amount of nitrogen entering the bioreactor by day 3. That means that for all experiments an extra input of nitrogen was brought to the water under the ionized forms NH_4^+, NO_2^- or NO_3^-. This finding is confirmed by the change in the electrical conductivity of the water recorded over time (Figure 6). As observed in each experiment, both curves depicting the direct measurement of EC_L on one y-axis and the total concentration in NH_4^+, NO_2^- and NO_3^- from ionic chromatography measurements on the other, follow a similar trend. It should be noted that, for each experiment, the dashed curve (EC_L) is not a modelled curve of the measured nitrogen concentration since curves are displayed according to two different y-axis. Consequently, the change in EC_L is entirely attributed to alterations in the concentrations of NH_4^+, NO_2^- and NO_3^- in the water, correlated with the nitrification process. The cumulative amounts of extra input reached 740±60, 330±30, 540±50 and 510±40 gN for EXP 1, 2, 3 and 4, respectively. Comparing the operating conditions across the four experiments reveals that the additional nitrogen input occurred after the onset of each experiment as soon as the pH decreased to 7.5±0.1. In the case of EXP 4, this input occurred at the beginning because the pH of the tap water used to replace the salty water at the end of EXP 3 was around 7.5±0.1. This prompts a legitimate inquiry into the origin of this nitrogen source.

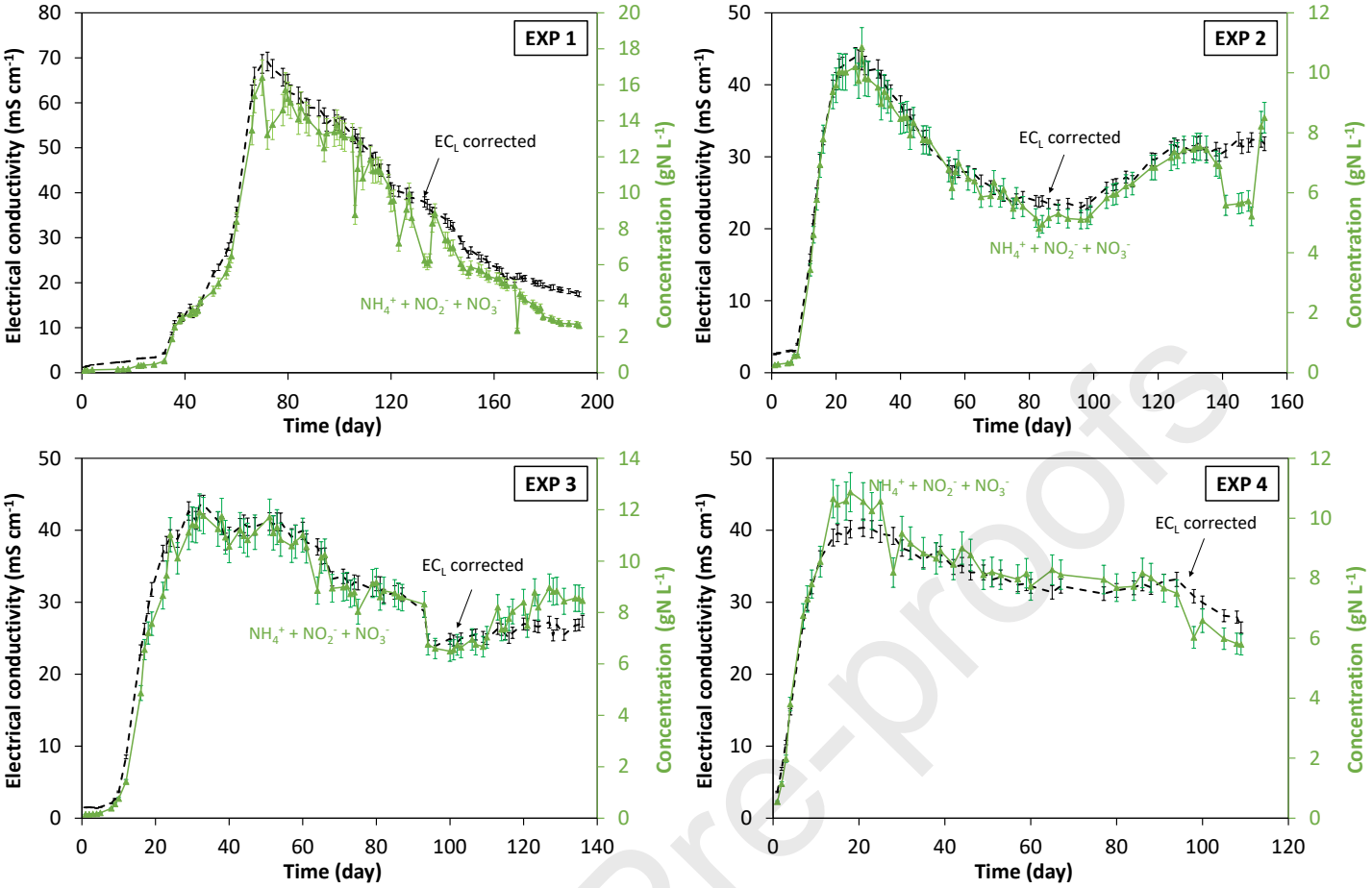

Figure 6 Change in nitrogen accumulation in the water over time (continuous line) due to ammonia mass transfer and nitrification ($NH_4^+ + NO_2^- + NO_3^-$; note that NO_3^- coming from tap water has been subtracted) compared with the change in the corrected electrical conductivity over time (dashed line; the corrected electrical conductivity values account for the cumulative addition of tap water over time)

Regarding the biomass, Figure 7 presents microbial diversity at the genus level based on NGS results for different samples collected in the bioreactor during EXP 3. The microbial community of the inoculum is primarily composed of genera such as *Haliangium*, *Thiothrix*, *Flavobacterium*, *Ferruginibacter*, *Tetrasphaera*, and *Terrimonas* genera. A wide range of OTUs identified in the inoculum are implicated in the nitrogen cycle, including denitrifiers and AOB. The low presence of AOB in the inoculum is consistent with literature data, indicating that 0.0033–0.33% of the bacteria in activated sludge from municipal sewage works are AOB [36]. After the acclimatization period of EXP 3 (12 days), sludge, biofilm and water sampled in the bioreactor were characterized over time. Sequence analyses highlighted changes in microbial communities over time, revealing three different patterns for sludge, water and biofilm. In the sludge sampled into the water tank, only a few OTUs from the inoculum were recovered in the microbial community, and 6 OTUs emerged from bacterial diversity analyses. It is noteworthy that a large part of the OTUs is associated with denitrifier metabolism, such as *Flavobacterium* and *Simplicispira*. Otherwise, minor changes in sludge patterns were observed over time. For the biofilm, genus level NGS analysis reveals that microbial patterns differed from the inoculum but were close to those in the sludge. The distribution of relative abundance between the samples was different, but the same OTUs were encountered in these two locations. Notably, on day 27, the abundance of AOB was high, with OTUs affiliated to *Nitrosomonas* and *Nitrospira* genera. This result is consistent with the high ammonia removal efficiency presented in Figure 2, especially between day 15 and day 30. After 69 days, no AOB were detected in the

biofilm, consistent with the low value of $RE_{measured}$ (around 6±3%). For the water, the microbial community change was sensitive over time. Twenty-seven days after the beginning, the community pattern was a mixture of both patterns encountered in the sludge and in the biofilm. AOB were detectable in the water, probably due to the bacterial biofilm transfer to the water. After 69 days until the end of experiment, the community changed, and only few OTUs dominated. NOB bacteria were not detected in any of the samples analyzed, aligning with the concentrations of FA and FNA, which might have led to NOB inhibition. Finally, Figure 7 suggests that bacteria involved in the biological oxidation of ammonia were present in the biofilm colonizing the packing material of the bioreactor. The three environments investigated in the bioreactor show similarities, particularly in their microbial composition, and many of the OTUs have a denitrifying metabolism.

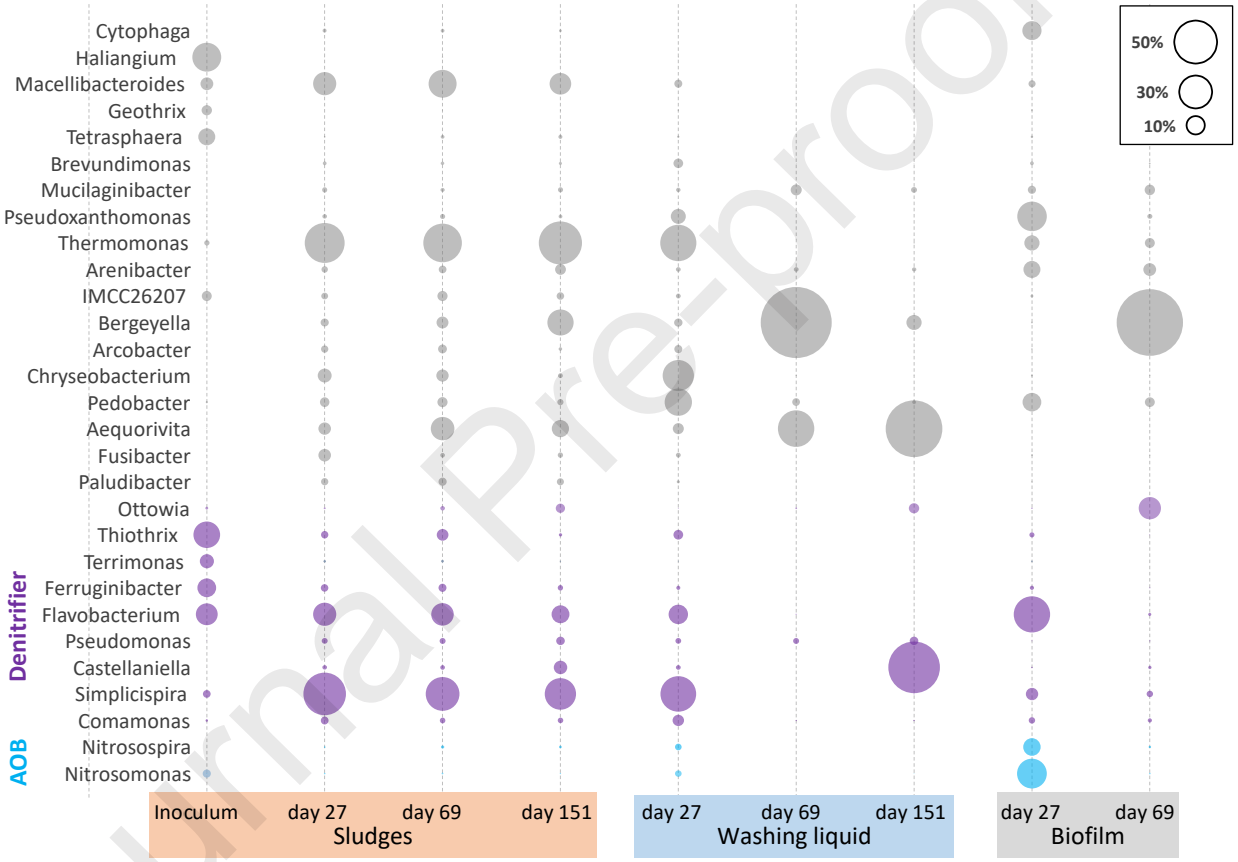

Figure 7 Results from next-generation sequencing (NGS) analysis at the genus level for microbial diversity within the bioreactor (EXP 3)

4. *Discussion*

The findings obtained during the four experiments showed that unexplained but reproducible phenomena occurred in the bioreactor: (1) loss of NH_4^+ and NO_2^- species in the water; (2) formation of NO_3^- despite the absence of NOB due to inhibition phenomena caused by high FA and FNA concentrations; (3) maintenance of the mass transfer of ammonia from the gas phase to the water concomitantly with the loss of NH_4^+ and NO_2^-; (4) unidentified extra inputs of ionized forms NH_4^+, NO_2^- and NO_3^- in the water of the bioreactor.

Before introducing possible mechanisms explaining these phenomena, it is important to keep in mind that all experiments were conducted under adverse conditions for biomass growth. NH_4^+ and NO_2^- concentrations reached up to several thousand mg L^{-1} (with no water renewal during each experiment), and no nutritive solution was added. Consequently, only inorganic compounds from the air (mainly NH_3 and CO_2) and tap water could be used by autotrophic bacteria to supplement their energy requirements. Nonetheless, the two inoculations with 10 L of activated sludge from a wastewater treatment plant, carried out at the beginning of EXP 1 and 3, represented two organic carbon additions that must be considered.

First of all, since various denitrifiers have been identified in the inoculum, as well as AOB *Nitrosomonas*, the large amount of NH_3 transferred from the gas phase during the acclimatization period of the biomass, in spite of unfavorable pH conditions, could be explained by complete denitrification since organic carbon from activated sludge inoculation was available. NH_3 would be transferred, oxidized, then reduced to N_2, and finally reemitted to the atmosphere. The conversion $NH_3 \rightarrow NH_4^+ \rightarrow N_2$ would maintain the ammonia driving force for mass transfer. Consequently, the bioreactor would act as an ammonia absorber with biochemical reaction, enhancing the rate of absorption and increasing the capacity of the water to dissolve ammonia compared with simple physical absorption [37]. This assumption would explain why the theoretical prediction of the NH_3 removal efficiency based on a simple physical absorption (Equation 7) is always slightly lower than the measured value, as the enhancement factor due to ammonia reaction was not considered in the theory [27]. Moreover, this assumption would also explain the contradictory effects observed during the decreasing phase of NH_4^+ and NO_2^- (EC_L decrease). Indeed, the bioreactor was capable to simultaneously absorbing NH_3 (RE was never nil and ranged between 6 and 20% according to the experiment, Figure 2) and removing NH_4^+ and NO_2^- from the water. This phenomena could contribute to the nitrogen imbalances reported in the literature dedicated to bioreactors treating ammonia emissions from piggeries [3,4,21]. However, microbial activities of nitrification and denitrification are a significant source of nitrous oxide (N_2O) to the atmosphere [38–43]. In the present study, N_2O production measured in the gas at the outlet of the bioreactor (Figure 1) was insignificant for the four experiments (0.5% of the NH_3 transferred from the gas), but a small production was detected in the air of the closed water tank. However, the air above the water in the tank represents a small volume that cannot leave the bioreactor. Consequently, in the absence of proof that N_2 has actually been reemitted into the atmosphere, we must remain very cautious about the direct conversion $NH_3 \rightarrow NH_4^+ \rightarrow N_2$ in the bioreactor.

The main issue is that the various denitrifiers identified in the inoculum were found in large proportions in the sludges, in the biofilm, and in the water throughout EXP 3 (Figure 7), even though there was no organic carbon addition. Denitrifying bacteria are facultative aerobic heterotrophs that switch from aerobic respiration to denitrification when oxygen is lacking. In the absence of oxygen, these microorganisms use NO_3^- as an electron acceptor. As a result, three conditions must be investigated to consider the presence of denitrifiers: (1) the lack of organic carbon, i.e., the C/N ratio; (2) the presence of NO_3^- despite the absence of NOB due to inhibition; and (3) the oxygen level in the bioreactor. First of all, during EXP 3, the total organic carbon measured in the water was 90±6 mg L^{-1}, and consequently, the C/N ratio < 1, since the amount of the ionic nitrogen forms reached several gN L^{-1} (Figure 3). Therefore, the amount of organic carbon was unfavorable to heterotrophic growth. Secondly, in the absence of NOB, the slow but continuous NO_3^- production all along the four experiments implies that nitrification still occurred in the water (Figure 3). Consequently, we have to conclude that NO_2^- was possibly oxidized into NO_3^- by heterotrophic bacteria despite the few available organic energy source [44]. In other words, simultaneous nitrification and denitrification (SND) possibly would occurred in the bioreactor at very low C/N ratio. According to the SND process, nitrification and denitrification reactions take place concomitantly in a single reactor, and there are several potential mechanisms for NO_2^- and NO_3^- production by heterotrophs [44]. Basically, SND would be due to a physical phenomenon characterized by a gradient of dissolved oxygen in the

microbial flocs affecting the activity of the nitrifiers and denitrifiers. Thus, the oxygen stratification in the aerobic biofilm creates micro-environments differing from the liquid bulk. Such micro-gradients of oxygen within an aerobic biofilm affecting the spatial distribution and rate of microbial processes were experimentally evidenced from microsensor analysis in a bioreactor treating ammonia emissions from piggeries [22]. Therefore, oxygen stratification possibly existed in the aerobic biofilm as well as in the sludges. Another potential mechanisms for NO_2^- and NO_3^- production by heterotrophs would be based on a macroenvironmental theory suggesting that nitrifiers and denitrifiers reside in the same reactor but at different locations according to the dissolved oxygen concentration [44]. The design of the bioreactor definitely promoted the formation of different macroenvironments since the biofilm fixed in the packing material directly contacted the air to be treated, whereas the sludges located at the bottom of the water tank were not in contact with the air flowing through the absorption column (Figure 1). Moreover, the water in the tank was not agitated, and its average residence time was 32 min for the operating conditions applied during the four experiments (Table 1), which is significantly higher than the contact time between air and water in the absorption column, around 2 s. The aeration of the water in the water tank was measured (dissolved oxygen concentrations ranged from 4.0 to 4.8±0.8 mg L^{-1}), but these values certainly did not reflect the potential oxygen stratification that could occur in the decanted sludges located at the bottom of the tank. A third mechanism, based on a micro-biological theory, implies that the nitrification reaction during SND is performed by two groups of micro-organisms: chemolithotrophic nitrifying AOB and heterotrophic nitrifiers present in the bioreactor. The latter are able to oxidize organic substrates in a co-metabolism reaction, involving the co-oxidation of either ammonia or reduced nitrogen from organic compounds, resulting in the formation of NO_2^- and NO_3^- [17,44]. In the bioreactor, organic compounds came from biomass growth via NH_4^+ assimilation [5,6], leading to biofilm formation. Biofilm consists of aggregates of cells embedded within a matrix of biopolymers called extracellular polymeric substances (EPS) [45]. The development of biofilm involves several successive steps: (i) initial contact with surfaces; (ii) irreversible attachment; (iii) microcolony formation; (iv) EPS synthesis; (v) maturation; (vi) detachment to disperse and move to new places for new colonization [45,46]. Consequently, dispersal, biofilm maturation, cell metabolism, and biomass decay continuously occur, leading to an accumulation of organic forms in the bioreactor. A part of these organic forms is represented by dissolved organic nitrogen (DON), which can serve as electron donors and/or nutrients sources for both autotrophs and heterotrophs. As an energy source, autotrophs can convert DON to ammonia, while as a nutrient source, DON can be hydrolyzed to small compounds (urea, amino acids,…) or directly assimilated [47]. Without the addition of organic carbon, it can be assumed that heterotrophs developed in the bioreactor due to the presence of DON from the biofilm formed by the autotrophs through NH_4^+ assimilation.

Given that satisfactory conditions for heterotrophic nitrification may have existed in the bioreactor (macroenvironments and microbiological theories), an attempt can be made to interpret the phenomena that occurred in the apparatus based on literature data [17,38,39,44,48,49]. In addition to NH_4^+ and NO_2^-, DON can also undergo oxidation. Moreover, heterotrophic bacteria can produce organic compounds containing oxidized nitrogen, and these compounds could serve as sources of NO_2^- and NO_3^- when decomposed. Some heterotrophic bacteria can simultaneously function as heterotrophic nitrifier (HN) and aerobic denitrifier (AD). The performance of these HN-AD bacteria, such as *Comamonas* and *Pseudomonas* isolated from various habitats, including saline wastewater [49], is influenced by several factors, mainly carbon and nitrogen sources, C/N ratio, oxygen, salinity and pH. Most HN-AD strains sharing similar physiological properties tend to thrive in a low C/N ratio (range of 8–10), under weak alkaline pH (7–9), low dissolved oxygen concentrations (<3 mg L^{-1}) and tolerate high NH_4^+ concentrations. These conditions matched those encountered in the bioreactor except for the detrimental C/N ratio <1. HN-AD bacteria convert inorganic or organic-containing substances into dinitrogen (N_2) through two pathways [50,51]: (1) $NH_4^+ \rightarrow NH_2OH \rightarrow NO_2^- \rightarrow NO_3^- \rightarrow NO_2^- \rightarrow NO \rightarrow N_2O \rightarrow N_2$ (NO_2^- and NO_3^- are observed to accumulate temporarily) and (2) $NH_4^+ \rightarrow NH_2OH \rightarrow NO \rightarrow N_2O \rightarrow N_2$ (hydroxylamine NH_2OH directly generates N_2 through denitrification).

Accordingly, the expected end-product of SND is N_2, but studies have demonstrated that NH_4^+ consumption can be also correlated with biomass propagation [52–54]. In other words, NH_4^+ is converted into biomass and the nitrogen forms NO_2^-, NO_3^- and N_2 are not necessarily produced during the process [53,55,56]. Ammonium removal rates reported in the literature by heterotrophs ranged from 5.5 to 93.2 mgN L^{-1} d^{-1} [52], which is within the order of magnitude of the values measured during the four experiments (Table 3). However, a sufficient carbon source is required to achieve efficient nitrogen removal through NH_4^+ assimilation. Between the two pathways $NH_3 \rightarrow NH_4^+ \rightarrow N_2$ and $NH_3 \rightarrow NH_4^+ \rightarrow$ biomass, one study argued from mass balance that approximately 55% of the NH_4^+ removed was lost as N_2, and 45% was assimilated (under the operating conditions C/N = 8, pH =7; NaCl = 3%, T = 30 °C [57]). In the present study, the N_2O production between the inlet and the outlet of the bioreactor (Figure 1) was insignificant for the four experiments, ruling out the pathway $NH_3 \rightarrow NH_4^+ \rightarrow N_2$ (except in the closed water tank where a marginal N_2O production was measured, as indicated above). With a C/N ratio < 1, the transformation of NH_3 into N_2 or biomass by heterotrophs is not expected. Consequently, in the absence of the evidence of N_2 production by the bioreactor and considering the low C/N ratio, we cannot conclude to the production of biomass rather than N_2 emission, and the SND track remains speculative.

Since the two nitrogen forms NH_4^+ and NO_2^- disappeared simultaneously at similar rates from the bioreactor, reactions between NH_4^+ and NO_2^- must also be considered. In a first approach, a possible biological anammox reaction ($NH_4^+ + NO_2^- \rightarrow N_2 + 2H_2O$) has been excluded since the bioreactor operated under aerobic conditions and with NH_4^+ and NO_2^- concentrations significantly higher than levels of inhibition reported in the literature [58,59]. Moreover, annamox bacteria were not detected in the bioreactor. In a second approach, a chemical reaction between NH_4^+ and NO_2^- in water is possible ($NH_4^+ + NO_2^- \rightarrow N_2 + 2H_2O$). The kinetics and mechanisms for a large range of pH and concentrations have been studied, but contradictory reaction orders and mechanisms were reported [60–65]. NH_4^+ and NO_2^-, as well as their derivatives $NH_{3,L}$ and HNO_2 forms, are used for mechanisms. According to Nguyen et al. [63], the reaction rate is $\mathrm{kC_{NH3}C_{HNO2}^2}$ and nitrosamine (H_2NNO) was determined as the most plausible intermediate leading to the final products. The reaction was found to be dependent on pH, exhibiting a 4000-fold increase as the pH decreased from 7 to 3. However, the potential mechanisms reported in the literature were investigated under acidic conditions. In the present case, the pH of the water was slightly higher than 7. Consequently, if a reaction occurred between NH_4^+ and NO_2^- via their derivatives $NH_{3,L}$ and HNO_2 forms, the reaction rate should be low. Furthermore, all attempts to fit the reaction rate, involving NH_4^+ and NO_2^- or/and their derivatives from experimental data, were unsuccessful. Additionally, since the same operating conditions were maintained during EXP 1-4, a physical reaction between NH_4^+ and NO_2^- would have resulted in similar removal rates for the four experiments, which was not observed (Table 3). Therefore, explaining the disappearance of the two nitrogen forms solely through an abiotic reaction between NH_4^+ and NO_2^- in water is challenging.

The extra inputs of nitrogen observed during the four experiments, clearly evidenced in Figure 4, must now be discussed. Despite an unfavorable C/N ratio, the rate of NH_4^+ removal during the phase of EC_L decrease (Figure 3) ranged from 27±2 mgN L^{-1} d^{-1} (EXP 4) to 56±5 mgN L^{-1} d^{-1} (EXP 1), which is in the order of magnitude of values reported in the literature dedicated to SND process [52]. However, considering that both NH_4^+ and NO_2^- were removed simultaneously at similar rates, and NO_3^- was produced concomitantly, the total nitrogen "lost" during this period ranged from 38±4 to 128±13 mgN L^{-1} d^{-1} (Table 3). As indicated above, this nitrogen "lost" was possibly partially used for biomass growth and partially reemitted to the atmosphere as N_2, although it is not possible to prove this definitively. Considering (i) the amount of nitrogen transferred from the gas to the water during the four experiments, (ii) the amount of nitrogen removed from the bioreactor due to water renewal between each experiment, (iii) the amount of nitrogen present in the bioreactor and the end of EXP 4 as NH_4^+, NO_2^- and NO_3^-, and (iv) the additional nitrogen supplies observed during experiments, it can be concluded that the part of nitrogen reemitted to the atmosphere was low compared to the

assimilated amount of nitrogen. Nitrite and nitrate can be produced by oxidation of ammonia and nitrogenous organic compounds through heterotrophic nitrification [17]. It is known that the microbial biomass production of heterotrophic bacteria is 40 times greater than the biomass formed from the nitrification process (8.06 g versus 0.20 g per g of NH_4^+-N converted into NO_3^--N [66]). Consequently, it is possible that the majority of the nitrogen transferred from the gas phase to the water was used for biomass growth, EPS, and DON production. The putative phenomena would be: once transferred from air to water, a large part of nitrogen would be entrapped in the bioreactor, evolving between inorganic forms (mainly NH_4^+, NO_2^-, and NO_3^-) and organic forms (mainly biomass, EPS, and DON). However, the change in the overall amounts of biomass in the bioreactor cannot be followed over time, and mechanisms controlling nitrogen distribution between inorganic and organic forms in the bioreactor are currently unresolved.

Based on the reproducible experimental results achieved during the four experiments and the literature data, potential mechanisms for nitrogen transformations between inorganic and organic forms in the bioreactor are summarized in Figure 8. Without liquid phase renewal, the water becomes loaded with ionic nitrogen species, and the nitrification process is clearly disturbed. Nitrogen assimilation/ammonification certainly plays a significant role in the bioreactor, but the adverse conditions characterized by a C/N ratio < 1 and large values of the electrical conductivity of water hamper the understanding of the biological autotrophic/heterotrophic phenomena that occurred.

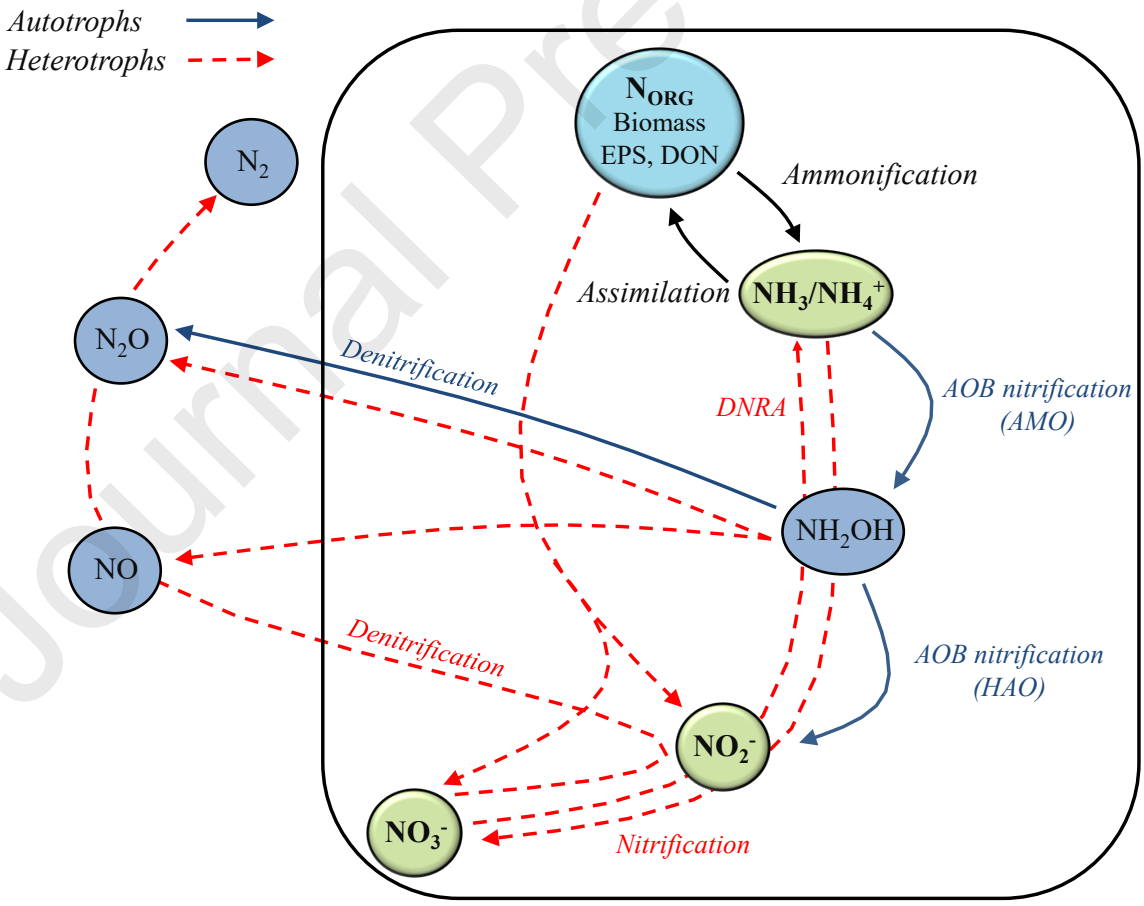

Figure 8 Potential microbial nitrogen transformations in the bioreactor performed by both autotrophic and heterotrophic nitrifiers (adapted from [17]). The presence of a black rectangle signifies predominant nitrogen entrapment within the bioreactor, with denitrification likely resulting in limited emissions of N_2O and N_2 (EPS: extracellular polymeric substances;

DON: dissolved organic nitrogen; DNRA: dissimilatory nitrate reduction to ammonium; AMO: ammonia monooxygenase; HAO: hydroxylamine oxidoreductase)

5. Conclusion

Unexpected but reproducible results emerged from four lengthy experiments conducted in a bioreactor designed to treat ammonia emissions under extreme conditions (without additional sources of nutrients or carbon). The continuous recirculation of water in the bioreactor led to the accumulation of nitrogen salts that disrupted the nitrification process. The most unexpected findings were (i) the simultaneous disappearance of NH_4^+ and NO_2^- species, despite a constant transfer of ammonia from the gas phase to the water, and (ii) the sudden appearance of unidentified inputs of inorganic nitrogen forms in the water (NH_4^+, NO_2^-, and NO_3^-), characterized by a notable increase in the electrical conductivity of the water.

From analysis of the bacterial community structures in the bioreactor, it was assumed that a simultaneous nitrification denitrification (SND) process occurred in the system. But it is possible that large amounts of nitrogen would be assimilated to generate organic compounds through ammonia assimilation. These compounds, in turn, would serve as a reservoir of available nitrogen through nitrogen ammonification. These findings attest that the significant nitrogen imbalances commonly observed in bioreactors treating NH_3 emissions, ascribed to denitrification processes, may also stem from nitrogen assimilation phenomena. Once transferred from gas to water, a large part of nitrogen would be entrapped in the bioreactor, evolving between inorganic forms, primarily NH_4^+, NO_2^-, and NO_3^-, and organic forms, predominantly biomass, extracellular polymeric substances (EPS), and dissolved organic nitrogen (DON). While the experimental results remain unquestionably valid, the credibility of these hypotheses is undermined by the low C/N ratio (<1) in the bioreactor, as well as the negligible N_2O production. The surprising phenomena recorded in the bioreactor remain unresolved and all assumptions remain to be proven. It is probable that certain microbial nitrification mechanisms are still unknown. The use of isotopic nitrogen in the bioreactor, coupled with enzyme activity and phylogenetic analyses in future work, will contribute to their elucidation. However, additional fundamental, small-scale researches will be needed to understand the observed phenomena.

Declaration of Competing Interest

The authors declare that they have no known competing financial interests or personal relationships that could have appeared to influence the work reported in this paper.

Acknowledgements

The authors would like to thank ADEME (N° TEZ19-041) and the Region of Brittany (N°1169) for their financial support.

CRediT author statement

Morgane POSER: methodology, resources, validation, formal analysis, investigation, data curation, writing—original draft preparation, writing—review and editing

Pascal PEU: validation, data curation, writing—review and editing, supervision

Annabelle COUVERT: conceptualization, validation, writing—review and editing, supervision, project administration, funding acquisition

Éric DUMONT: conceptualization, methodology, data curation, validation, writing—original draft preparation, writing—review and editing, supervision

References

[1] É. Dumont, S. Lagadec, N. Guingand, L. Loyon, A. Amrane, V. Couroussé, A. Couvert, Ammonia Removal Using Biotrickling Filters: Part A: Determination of the Ionic Nitrogen Concentration of Water Using Electrical Conductivity Measurement, ChemEngineering. 4 (2020) 49. https://doi.org/10.3390/chemengineering4030049.

[2] F. Liu, C. Fiencke, J. Guo, R. Rieth, C. Cuhls, R. Dong, E.-M. Pfeiffer, Bioscrubber treatment of exhaust air from intensive pig production: Case study in northern Germany at mild climate condition, Eng. Life Sci. 17 (2017) 458–466. https://doi.org/10.1002/elsc.201600169.

[3] R.W. Melse, J.P.M. Ploegaert, N.W.M. Ogink, Biotrickling filter for the treatment of exhaust air from a pig rearing building: Ammonia removal performance and its fluctuations, Biosyst. Eng. 113 (2012) 242–252. https://doi.org/10.1016/j.biosystemseng.2012.08.010.

[4] C. Van der Heyden, E.I.P. Volcke, E. Brusselman, P. Demeyer, Comparative 1-year performance study of two full-scale biotrickling filters for ammonia removal including nitrous oxide emission monitoring, Biosyst. Eng. 188 (2019) 178–189. https://doi.org/10.1016/j.biosystemseng.2019.10.014.

[5] R. Hu, S. Liu, W. Huang, Q. Nan, P.J. Strong, M. Saleem, Z. Zhou, Z. Luo, F. Shu, Q. Yan, Z. He, C. Wang, Evidence for Assimilatory Nitrate Reduction as a Previously Overlooked Pathway of Reactive Nitrogen Transformation in Estuarine Suspended Particulate Matter, Environ. Sci. Technol. 56 (2022) 14852–14866. https://doi.org/10.1021/acs.est.2c04390.

[6] X. Cai, R. Liu, M. Cheng, T. Liu, Y. Zhang, X. Li, Y. Zeng, H. Long, W. Ren, Z. Xie, Characterization of a novel Pseudomonas mosselii 9-1 capable of nitrate reduction to ammonium, ammonium assimilation, and denitrification in aerobic conditions, J. Water Process Eng. 52 (2023) 103531. https://doi.org/10.1016/j.jwpe.2023.103531.

[7] É. Dumont, S. Lagadec, N. Guingand, L. Loyon, A. Amrane, A. Couvert, Ammonia Removal Using Biotrickling Filters: Part B: Determination of the Nitrogen Accumulation in the Scrubbing Liquid at a Livestock Facility Using Electrical Conductivity Measurement, ChemEngineering. 4 (2020) 50. https://doi.org/10.3390/chemengineering4030050.

[8] L. Tang, M.A. Deshusses, Novel Integrated Biotrickling Filter–Anammox Bioreactor System for the Complete Treatment of Ammonia in Air with Nitrification and Denitrification, Environ. Sci. Technol. 54 (2020) 12654–12661. https://doi.org/10.1021/acs.est.0c03332.

[9] A.C. Anthonisen, R.C. Loehr, T.B.S. Prakasam, E.G. Srinath, Inhibition of Nitrification by Ammonia and Nitrous Acid, J. Water Pollut. Control Fed. 48 (1976) 835–852.

[10] F. Zhang, H. Yang, J. Wang, Z. Liu, Q. Guan, Effect of free ammonia inhibition on NOB activity in high nitrifying performance of sludge, RSC Adv. 8 (2018) 31987–31995. https://doi.org/10.1039/C8RA06198J.

[11] V.M. Vadivelu, J. Keller, Z. Yuan, Effect of free ammonia and free nitrous acid concentration on the anabolic and catabolic processes of an enrichedNitrosomonas culture, Biotechnol. Bioeng. 95 (2006) 830–839. https://doi.org/10.1002/bit.21018.

[12] Q. Wang, H. Duan, W. Wei, B.-J. Ni, A. Laloo, Z. Yuan, Achieving Stable Mainstream Nitrogen Removal via the Nitrite Pathway by Sludge Treatment Using Free Ammonia, Environ. Sci. Technol. 51 (2017) 9800–9807. https://doi.org/10.1021/acs.est.7b02776.

[13] Y. Liu, H.H. Ngo, W. Guo, L. Peng, D. Wang, B. Ni, The roles of free ammonia (FA) in biological wastewater treatment processes: A review, Environ. Int. 123 (2019) 10–19. https://doi.org/10.1016/j.envint.2018.11.039.

[14] L.D.M. Ottosen, S. Juhler, L.B. Guldberg, A. Feilberg, N.P. Revsbech, L.P. Nielsen, Regulation of ammonia oxidation in biotrickling airfilters with high ammonium load, Chem. Eng. J. 167 (2011) 198–205. https://doi.org/10.1016/j.cej.2010.12.022.

[15] A. Soler-Jofra, J. Pérez, M.C.M. van Loosdrecht, Hydroxylamine and the nitrogen cycle: A review, Water Res. 190 (2021) 116723. https://doi.org/10.1016/j.watres.2020.116723.

[16] G. Zhu, X. Wang, S. Wang, L. Yu, G. Armanbek, J. Yu, L. Jiang, D. Yuan, Z. Guo, H. Zhang, L. Zheng, L. Schwark, M.S.M. Jetten, A.K. Yadav, Y.-G. Zhu, Towards a more labor-saving way in microbial ammonium oxidation: A review on complete ammonia oxidization (comammox), Sci. Total Environ. 829 (2022) 154590. https://doi.org/10.1016/j.scitotenv.2022.154590.

[17] P.J. Martikainen, Heterotrophic nitrification – An eternal mystery in the nitrogen cycle, Soil Biol. Biochem. 168 (2022) 108611. https://doi.org/10.1016/j.soilbio.2022.108611.

[18] K. Calvin, D. Dasgupta, G. Krinner, A. Mukherji, P.W. Thorne, C. Trisos, J. Romero, P. Aldunce, K. Barrett, G. Blanco, W.W.L. Cheung, S. Connors, F. Denton, A. Diongue-Niang, D. Dodman, M. Garschagen, O. Geden, B. Hayward, C. Jones, F. Jotzo, T. Krug, R. Lasco, Y.-Y. Lee, V. Masson-Delmotte, M. Meinshausen, K. Mintenbeck, A. Mokssit, F.E.L. Otto, M. Pathak, A. Pirani, E. Poloczanska, H.-O. Pörtner, A. Revi, D.C. Roberts, J. Roy, A.C. Ruane, J. Skea, P.R. Shukla, R. Slade, A. Slangen, Y. Sokona, A.A. Sörensson, M. Tignor, D. Van Vuuren, Y.-M. Wei, H. Winkler, P. Zhai, Z. Zommers, J.-C. Hourcade, F.X. Johnson, S. Pachauri, N.P. Simpson, C. Singh, A. Thomas, E. Totin, P. Arias, M. Bustamante, I. Elgizouli, G. Flato, M. Howden, C. Méndez-Vallejo, J.J. Pereira, R. Pichs-Madruga, S.K. Rose, Y. Saheb, R. Sánchez Rodríguez, D. Ürge-Vorsatz, C. Xiao, N. Yassaa, A. Alegría, K. Armour, B. Bednar-Friedl, K. Blok, G. Cissé, F. Dentener, S. Eriksen, E. Fischer, G. Garner, C. Guivarch, M. Haasnoot, G. Hansen, M. Hauser, E. Hawkins, T. Hermans, R. Kopp, N. Leprince-Ringuet, J. Lewis, D. Ley, C. Ludden, L. Niamir, Z. Nicholls, S. Some, S. Szopa, B. Trewin, K.-I. Van Der Wijst, G. Winter, M. Witting, A. Birt, M. Ha, J. Romero, J. Kim, E.F. Haites, Y. Jung, R. Stavins, A. Birt, M. Ha, D.J.A. Orendain, L. Ignon, S. Park, Y. Park, A. Reisinger, D. Cammaramo, A. Fischlin, J.S. Fuglestvedt, G. Hansen, C. Ludden, V. Masson-Delmotte, J.B.R. Matthews, K. Mintenbeck, A. Pirani, E. Poloczanska, N. Leprince-Ringuet, C. Péan, IPCC, 2023: Climate Change 2023: Synthesis Report. Contribution of Working Groups I, II and III to the Sixth Assessment Report of the Intergovernmental Panel on Climate Change [Core Writing Team, H.

Lee and J. Romero (eds.)]. IPCC, Geneva, Switzerland., First, Intergovernmental Panel on Climate Change (IPCC), 2023. https://doi.org/10.59327/IPCC/AR6-9789291691647.

[19] C. Van der Heyden, E. Brusselman, E.I.P. Volcke, P. Demeyer, Continuous measurements of ammonia, nitrous oxide and methane from air scrubbers at pig housing facilities, J. Environ. Manage. 181 (2016) 163–171. https://doi.org/10.1016/j.jenvman.2016.06.006.

[20] L. Loyon, P. Dupard, P. Saint-Cast, F. Guiziou, Assessment of NH3 Reduction and N2O Production during Treatment of Exhausted Air from Fattening Pigs Building by a Commercial Scrubber, Agric. Sci. 07 (2016) 693. https://doi.org/10.4236/as.2016.710065.

[21] E. Blázquez, T. Bezerra, J. Lafuente, D. Gabriel, Performance, limitations and microbial diversity of a biotrickling filter for the treatment of high loads of ammonia, Chem. Eng. J. 311 (2017) 91–99. https://doi.org/10.1016/j.cej.2016.11.072.

[22] S. Juhler, N.P. Revsbech, A. Schramm, M. Herrmann, L.D.M. Ottosen, L.P. Nielsen, Distribution and Rate of Microbial Processes in an Ammonia-Loaded Air Filter Biofilm, Appl. Environ. Microbiol. 75 (2009) 3705–3713. https://doi.org/10.1128/AEM.02612-08.

[23] B.B. Colliver, T. Stephenson, Production of nitrogen oxide and dinitrogen oxide by autotrophic nitrifiers, Biotechnol. Adv. 18 (2000) 219–232. https://doi.org/10.1016/S0734-9750(00)00035-5.

[24] S. Lv, F. Zheng, Z. Wang, K. Hayat, M.C. Veiga, C. Kennes, J. Chen, Unveiling novel pathways and key contributors in the nitrogen cycle: Validation of enrichment and taxonomic characterization of oxygenic denitrifying microorganisms in environmental samples, Sci. Total Environ. 908 (2024) 168339. https://doi.org/10.1016/j.scitotenv.2023.168339.

[25] D. Li, X. Liang, C. Wu, Characteristics of Nitrogen Removal and Extracellular Polymeric Substances of a Novel Salt-Tolerant Denitrifying Bacterium, Pseudomonas sp. DN-23, Front. Microbiol. 11 (2020) 335. https://doi.org/10.3389/fmicb.2020.00335.

[26] R. Sander, Compilation of Henry's law constants (version 4.0) for water as solvent, Atmospheric Chem. Phys. 15 (2015) 4399–4981. https://doi.org/10.5194/acp-15-4399-2015.

[27] E. Dumont, M. Poser, P. Peu, A. Couvert, Biotrickling filters for the removal of gaseous ammonia emissions from livestock facilities. Theoretical prediction of removal efficiency and experimental validation, Chem. Eng. J. 402 (2020) 126188. https://doi.org/10.1016/j.cej.2020.126188.

[28] C. Madigou, K.-A. Lê Cao, C. Bureau, L. Mazéas, S. Déjean, O. Chapleur, Ecological consequences of abrupt temperature changes in anaerobic digesters, Chem. Eng. J. 361 (2019) 266–277. https://doi.org/10.1016/j.cej.2018.12.003.

[29] Y. Wang, P.-Y. Qian, Conservative Fragments in Bacterial 16S rRNA Genes and Primer Design for 16S Ribosomal DNA Amplicons in Metagenomic Studies, PLoS ONE. 4 (2009) e7401. https://doi.org/10.1371/journal.pone.0007401.

[30] F. Escudié, L. Auer, M. Bernard, M. Mariadassou, L. Cauquil, K. Vidal, S. Maman, G. Hernandez-Raquet, S. Combes, G. Pascal, FROGS: Find, Rapidly, OTUs with Galaxy Solution, Bioinformatics. 34 (2018) 1287–1294. https://doi.org/10.1093/bioinformatics/btx791.

[31] P.J. McMurdie, S. Holmes, phyloseq: An R Package for Reproducible Interactive Analysis and Graphics of Microbiome Census Data, PLoS ONE. 8 (2013) e61217. https://doi.org/10.1371/journal.pone.0061217.

[32] M. Kanehisa, S. Goto, KEGG: kyoto encyclopedia of genes and genomes, Nucleic Acids Res. 28 (2000) 27–30. https://doi.org/10.1093/nar/28.1.27.

[33] W. Pongkua, P. Thiravetyan, E. Dumont, New tool for the determination of the nitrogen accumulation rate in the washing liquid of a biotrickling filter treating ammonia emissions, Chem. Eng. J. 397 (2020) 125399. https://doi.org/10.1016/j.cej.2020.125399.

[34] V.M. Vadivelu, J. Keller, Z. Yuan, Free ammonia and free nitrous acid inhibition on the anabolic and catabolic processes of Nitrosomonas and Nitrobacter, Water Sci. Technol. 56 (2007) 89–97. https://doi.org/10.2166/wst.2007.612.

[35] M.S. Pourbavarsad, B.J. Jalalieh, N. Landes, W.A. Jackson, Impact of free ammonia and free nitrous acid on nitritation in membrane aerated bioreactors fed with high strength nitrogen urine dominated wastewater, J. Environ. Chem. Eng. 10 (2022) 107001. https://doi.org/10.1016/j.jece.2021.107001.

[36] G. Harms, A.C. Layton, H.M. Dionisi, I.R. Gregory, V.M. Garrett, S.A. Hawkins, K.G. Robinson, G.S. Sayler, Real-time PCR quantification of nitrifying bacteria in a municipal wastewater treatment plant, Environ. Sci. Technol. 37 (2003) 343–351. https://doi.org/10.1021/es0257164.

[37] J. Fair, D. Steinmeyer, W. Penney, B. Corcker, Gas absorption and gas-liquid system design, in: Perrys Chem. Eng. Handb. Eighth Ed. Perry RH Green DW Ed., 8th ed., McGraw-Hill, 2008: pp. 14-1 14-98.

[38] L.Y. Stein, Heterotrophic Nitrification and Nitrifier Denitrification, in: B.B. Ward, D.J. Arp, M.G. Klotz (Eds.), Nitrification, ASM Press, Washington, DC, USA, 2014: pp. 95–114. https://doi.org/10.1128/9781555817145.ch5.

[39] F. Di Capua, F. Iannacone, F. Sabba, G. Esposito, Simultaneous nitrification–denitrification in biofilm systems for wastewater treatment: Key factors, potential routes, and engineered applications, Bioresour. Technol. 361 (2022) 127702. https://doi.org/10.1016/j.biortech.2022.127702.

[40] L.C. Valk, M. Peces, C.M. Singleton, M.D. Laursen, M.H. Andersen, A.T. Mielczarek, P.H. Nielsen, Exploring the microbial influence on seasonal nitrous oxide concentration in a full-scale wastewater treatment plant using metagenome assembled genomes, Water Res. 219 (2022) 118563. https://doi.org/10.1016/j.watres.2022.118563.

[41] M.J. Kampschreur, H. Temmink, R. Kleerebezem, M.S.M. Jetten, M.C.M. van Loosdrecht, Nitrous oxide emission during wastewater treatment, Water Res. 43 (2009) 4093–4103. https://doi.org/10.1016/j.watres.2009.03.001.

[42] Z. Li, X. Yang, H. Chen, M. Du, Y.S. Ok, Modeling nitrous oxide emissions in membrane bioreactors: Advancements, challenges and perspectives, Sci. Total Environ. 806 (2022) 151394. https://doi.org/10.1016/j.scitotenv.2021.151394.

[43] L.J. Shaw, G.W. Nicol, Z. Smith, J. Fear, J.I. Prosser, E.M. Baggs, Nitrosospira spp. can produce nitrous oxide via a nitrifier denitrification pathway, Environ. Microbiol. 8 (2006) 214–222. https://doi.org/10.1111/j.1462-2920.2005.00882.x.

[44] R.K. Gupta, B.J. Poddar, S.P. Nakhate, A.R. Chavan, A.K. Singh, H.J. Purohit, A.A. Khardenavis, Role of heterotrophic nitrifiers and aerobic denitrifiers in simultaneous nitrification and denitrification process: a nonconventional nitrogen removal pathway in wastewater treatment, Lett. Appl. Microbiol. 74 (2022) 159–184. https://doi.org/10.1111/lam.13553.

[45] K.U. Mahto, S. Das, Bacterial biofilm and extracellular polymeric substances in the moving bed biofilm reactor for wastewater treatment: A review, Bioresour. Technol. 345 (2022) 126476. https://doi.org/10.1016/j.biortech.2021.126476.

[46] A.H. Jagaba, S.R.M. Kutty, A. Noor, A.H. Birniwa, A.C. Affam, I.M. Lawal, M.U. Kankia, A.U. Kilaco, A systematic literature review of biocarriers: Central elements for biofilm formation, organic and nutrients removal in sequencing batch biofilm reactor, J. Water Process Eng. 42 (2021) 102178. https://doi.org/10.1016/j.jwpe.2021.102178.

[47] F. Zheng, J. Wang, R. Xiao, W. Chai, D. Xing, H. Lu, Dissolved organic nitrogen in wastewater treatment processes: Transformation, biosynthesis and ecological impacts, Environ. Pollut. 273 (2021) 116436. https://doi.org/10.1016/j.envpol.2021.116436.

[48] W. Ma, Y. Han, W. Ma, H. Han, H. Zhu, C. Xu, K. Li, D. Wang, Enhanced nitrogen removal from coal gasification wastewater by simultaneous nitrification and denitrification (SND) in an oxygen-limited aeration sequencing batch biofilm reactor, Bioresour. Technol. 244 (2017) 84–91. https://doi.org/10.1016/j.biortech.2017.07.083.

[49] H. Xi, X. Zhou, M. Arslan, Z. Luo, J. Wei, Z. Wu, M. Gamal El-Din, Heterotrophic nitrification and aerobic denitrification process: Promising but a long way to go in the wastewater treatment, Sci. Total Environ. 805 (2022) 150212. https://doi.org/10.1016/j.scitotenv.2021.150212.

[50] X. Liu, Q. Zhang, X. Yang, D. Wu, Y. Li, H. Di, Isolation and characteristics of two heterotrophic nitrifying and aerobic denitrifying bacteria, Achromobacter sp. strain HNDS-1 and Enterobacter sp. strain HNDS-6, Environ. Res. 220 (2023) 115240. https://doi.org/10.1016/j.envres.2023.115240.

[51] Y. Yan, H. Lu, J. Zhang, S. Zhu, Y. Wang, Y. Lei, R. Zhang, L. Song, Simultaneous heterotrophic nitrification and aerobic denitrification (SND) for nitrogen removal: A review and future perspectives, Environ. Adv. 9 (2022) 100254. https://doi.org/10.1016/j.envadv.2022.100254.

[52] F. Han, W. Zhou, Nitrogen recovery from wastewater by microbial assimilation – A review, Bioresour. Technol. 363 (2022) 127933. https://doi.org/10.1016/j.biortech.2022.127933.

[53] Y. Sun, L. Feng, A. Li, X. Zhang, J. Yang, F. Ma, Ammonium assimilation: An important accessory during aerobic denitrification of Pseudomonas stutzeri T13, Bioresour. Technol. 234 (2017) 264–272. https://doi.org/10.1016/j.biortech.2017.03.053.

[54] M. Zhang, F. Han, Y. Li, Z. Liu, H. Chen, Z. Li, Q. Li, W. Zhou, Nitrogen recovery by a halophilic ammonium-assimilating microbiome: A new strategy for saline wastewater treatment, Water Res. 207 (2021) 117832. https://doi.org/10.1016/j.watres.2021.117832.

[55] M. Zhang, F. Han, Z. Liu, Y. Han, Y. Li, W. Zhou, Ammonium-assimilating microbiome: A halophilic biosystem rationally optimized by carbon to nitrogen ratios with stable nitrogen conversion and microbial structure, Bioresour. Technol. 350 (2022) 126911. https://doi.org/10.1016/j.biortech.2022.126911.

[56] Y. Li, Y. Wang, L. Fu, Y. Gao, H. Zhao, W. Zhou, Aerobic-heterotrophic nitrogen removal through nitrate reduction and ammonium assimilation by marine bacterium Vibrio sp. Y1-5, Bioresour. Technol. 230 (2017) 103–111. https://doi.org/10.1016/j.biortech.2017.01.049.

[57] L. Carneiro Fidélis Silva, H. Santiago Lima, T. Antônio de Oliveira Mendes, A. Sartoratto, M. de Paula Sousa, R. Suhett de Souza, S. Oliveira de Paula, V. Maia de Oliveira, C. Canêdo da Silva, Heterotrophic nitrifying/aerobic denitrifying bacteria: Ammonium removal under different physical-chemical conditions and molecular characterization, J. Environ. Manage. 248 (2019) 109294. https://doi.org/10.1016/j.jenvman.2019.109294.

[58] A.S. Arora, A. Nawaz, M.A. Qyyum, S. Ismail, M. Aslam, A. Tawfik, C.M. Yun, M. Lee, Energy saving anammox technology-based nitrogen removal and bioenergy recovery from wastewater: Inhibition mechanisms, state-of-the-art control strategies, and prospects, Renew. Sustain. Energy Rev. 135 (2021) 110126. https://doi.org/10.1016/j.rser.2020.110126.

[59] L. Sheng, Z. Lei, M. Dzakpasu, Y.-Y. Li, Q. Li, R. Chen, Application of the anammox-based process for nitrogen removal from anaerobic digestion effluent: A review of treatment performance, biochemical reactions, and impact factors, J. Water Process Eng. 38 (2020) 101595. https://doi.org/10.1016/j.jwpe.2020.101595.

[60] T. Bryant, D.L.H. Williams, Nitrosation of ammonia, J. Chem. Soc. Perkin Trans. 2. (1988) 97. https://doi.org/10.1039/p29880000097.

[61] G.D. Silva, B.Z. Dlugogorski, E.M. Kennedy, Elementary reaction step model of the N-nitrosation of ammonia, Int. J. Chem. Kinet. 39 (2007) 645–656. https://doi.org/10.1002/kin.20280.

[62] J.H. Dusenbury, R.E. Powell, Reactions of Nitrous Acid. I. Ammonium Nitrite Decomposition [1], J. Am. Chem. Soc. 73 (1951) 3266–3268. https://doi.org/10.1021/ja01151a080.

[63] D.A. Nguyen, M.A. Iwaniw, H.S. Fogler, Kinetics and mechanism of the reaction between ammonium and nitrite ions: experimental and theoretical studies, Chem. Eng. Sci. 58 (2003) 4351–4362. https://doi.org/10.1016/S0009-2509(03)00317-8.

[64] C.C. Harrison, M.A. Malati, N.B. Smetham, The UV-enhanced decomposition of aqueous ammonium nitrite, J. Photochem. Photobiol. Chem. 89 (1995) 215–219. https://doi.org/10.1016/1010-6030(95)04060-S.

[65] C.C. Harrison, M.A. Malati, N.B. Smetham, Solvent and deuterium isotope effects on the decomposition of ammonium nitrite solutions, J. Solut. Chem. 25 (1996) 505–514. https://doi.org/10.1007/BF00972995.

[66] J.M. Ebeling, M.B. Timmons, J.J. Bisogni, Engineering analysis of the stoichiometry of photoautotrophic, autotrophic, and heterotrophic removal of ammonia–nitrogen in aquaculture systems, Aquaculture. 257 (2006) 346–358. https://doi.org/10.1016/j.aquaculture.2006.03.019.

Highlights

Four similar studies explored nitrification in waters with elevated nitrogen salts

Accumulation of nitrogen salts in water disrupts the nitrification process

Nitrogen transformations would be due to heterotrophs despite adverse C/N ratio

Despite clear results, disturbances in nitrification remain unresolved